UNIVERSIDAD DE INVESTIGACIÓN DE TECNOLOGÍA EXPERIMENTAL YACHAY

Escuela de ciencias Físicas y Nanotecnología

TÍTULO: RAMAN SPECTROSCOPY IN ANCIENT MATERIALS

Trabajo de integración curricular presentado como requisito para la obtención del título de Físico.

Author:
Quezada Villarreal Christopher Jhoanpier

Advisor:
Dr. rer. nat. Chacón Torres Julio Cesar

Urcuquí, enero de 2023

UNIVERSIDAD
YACHAY
TECH

Urcuquí, 21 de noviembre de 2022

SECRETARÍA GENERAL
ESCUELA DE CIENCIAS FÍSICAS Y NANOTECNOLOGÍA
CARRERA DE FÍSICA
ACTA DE DEFENSA No. UITEY-PHY-2022-00022-AD

En la ciudad de San Miguel de Urcuquí, Provincia de Imbabura, a los 21 días del mes de noviembre de 2022, a las 14:30 horas, en el Aula S_CAN de la Universidad de Investigación de Tecnología Experimental Yachay y ante el Tribunal Calificador, integrado por los docentes:

Presidente Tribunal de Defensa	Dr. REINOSO CARLOS , Ph.D.
Miembro No Tutor	LAGOS LLAGUNO, DANIEL ALEJANDRO , Ph.D.
Tutor	Dr. CHACON TORRES, JULIO CESAR , Ph.D.

Se presenta el(la) señor(ita) estudiante **QUEZADA VILLARREAL, CHRISTOPHER JHOANPIER**, con cédula de identidad No. **2100661871**, de la **ESCUELA DE CIENCIAS FÍSICAS Y NANOTECNOLOGÍA**, de la Carrera de **FÍSICA**, aprobada por el Consejo de Educación Superior (CES), mediante Resolución **RPC-SO-39-No.456-2014**, con el objeto de rendir la sustentación de su trabajo de titulación denominado: **Raman spectroscopy in ancient materials** , previa a la obtención del título de **FÍSICO/A**.

El citado trabajo de titulación, fue debidamente aprobado por el(los) docente(s):

Tutor	Dr. CHACON TORRES, JULIO CESAR , Ph.D.

Y recibió las observaciones de los otros miembros del Tribunal Calificador, las mismas que han sido incorporadas por el(la) estudiante.

Previamente cumplidos los requisitos legales y reglamentarios, el trabajo de titulación fue sustentado por el(la) estudiante y examinado por los miembros del Tribunal Calificador. Escuchada la sustentación del trabajo de titulación, que integró la exposición de el(la) estudiante sobre el contenido de la misma y las preguntas formuladas por los miembros del Tribunal, se califica la sustentación del trabajo de titulación con las siguientes calificaciones:

Tipo	Docente	Calificación
Miembro Tribunal De Defensa	LAGOS LLAGUNO, DANIEL ALEJANDRO , Ph.D.	8,6
Tutor	Dr. CHACON TORRES, JULIO CESAR , Ph.D.	9,0
Presidente Tribunal De Defensa	Dr. REINOSO CARLOS , Ph.D.	9,0

Lo que da un promedio de: **8.9 (Ocho punto Nueve)**, sobre 10 (diez), equivalente a: **APROBADO**

Para constancia de lo actuado, firman los miembros del Tribunal Calificador, el/la estudiante y el/la secretario ad-hoc.

QUEZADA VILLARREAL, CHRISTOPHER JHOANPIER
Estudiante

Dr. REINOSO CARLOS , Ph.D.
Presidente Tribunal de Defensa

Dr. CHACON TORRES, JULIO CESAR , Ph.D.
Tutor

LAGOS LLAGUNO, DANIEL ALEJANDRO , Ph.D.
Miembro No Tutor

CIFUENTES TAFUR, EVELYN CAROLINA
Secretario Ad-hoc

AUTORÍA

Yo, Christopher Jhoanpier Quezada Villarreal, con cédula de identidad 2100661871, declaro que las ideas, juicios, valoraciones, interpretaciones, consultas bibliográficas, definiciones y conceptualizaciones expuestas en el presente trabajo; así cómo, los procedimientos y herramientas utilizadas en la investigación, son de absoluta responsabilidad de el/la autora (a) del trabajo de integración curricular.

Así mismo, me acojo a los reglamentos internos de la Universidad de Investigación de Tecnología Experimental Yachay.

Urcuquí, Enero de 2023.

CHRISTOPHER
JHOANPIER
QUEZADA
VILLARREAL

Firmado digitalmente
por CHRISTOPHER
JHOANPIER QUEZADA
VILLARREAL
Fecha: 2023.01.12
10:39:10 -05'00'

Christopher Jhoanpier Quezada Villarreal
CI: 2100661871

AUTORIZACIÓN DE PUBLICACIÓN

Yo, Christopher Jhoanpier Quezada Villarreal, con cédula de identidad 2100661871, cedo a la Universidad de Tecnología Experimental Yachay, los derechos de publicación de la presente obra, sin que deba haber un reconocimiento económico por este concepto. Declaro además que el texto del presente trabajo de titulación no podrá ser cedido a ninguna empresa editorial para su publicación u otros fines, sin contar previamente con la autorización escrita de la Universidad.

Asimismo, autorizo a la Universidad que realice la digitalización y publicación de este trabajo de integración curricular en el repositorio virtual, de conformidad a lo dispuesto en el Art. 144 de la Ley Orgánica de Educación Superior.

Urcuquí, Enero de 2023.

CHRISTOPHER JHOANPIER QUEZADA VILLARREAL

Firmado digitalmente por CHRISTOPHER JHOANPIER QUEZADA VILLARREAL
Fecha: 2023.01.12 10:42:50 -05'00'

____

Christopher Jhoanpier Quezada Villarreal
CI: 2100661871

Acknowledgements

I would like to express my gratitude to the PhD. Julio Chacón who was an important pillar in the development of this work. My gratitude began when he agreed to work with me on a topic so different from others, but no less important. I appreciate having the opportunity to develop a research work that motivates me. This process has been one of the most enriching experiences in my professional and personal life. This work has been a fundamental part of my development as a student and has allowed me to take a direction in my future as a researcher. I unquestionably owe this to my thesis advisor who knew how to personally understand the interest I have in developing studies in these fields. I also appreciate that my advisor had the patience and time to conduct these analyzes in Berlin. I think that one of the most important things in teaching is to teach through the perspective of curiosity and interest. Thank you very much to all Yachay Tech teachers who instill curiosity in students, I believe it is essential for the development of good professional human beings. Thanks to the advice that certain people gave me when I was in trouble. Many thanks to my classmates who were friends and supports. A special thanks to El Nido, an academic space, in particular to Professor Yadira Gallegos and her mother Rosa Isabel Gallegos Calderón who provided us with vessels A and B. Also, thanks to La TOLA Centro de Arte y Cultura, in particular Francisco and his family who provided us with vessels C and D. A special thanks to Maria Elena Villarreal and Franklin Quezada, my parents. I want to dedicate this work to my parents and also thank them for all the sacrifices they have made.

Christopher Jhoanpier Quezada Villarreal

Resumen

La espectroscopia de Raman ha creado un nicho en el campo del diagnóstico, análisis y conservación del patrimonio cultural y de diferentes obras artísticas como los objetos arqueológicos. Esta técnica de Arqueometría nos permite mejorar la preservación de lod diferentes objetos que forman parte del patrimonio cultural del Ecuador y el estudio de las propiedades estructurales de los materiales que los componen. Sin embargo, un desafío importante para los investigadores es la evaluación adecuada de la procedencia y la composición química y estructural de estas piezas debido a la falta de estudios arqueológicos y técnicas de caracterización avanzadas. La espectroscopia de Raman es una técnica precisa no destructiva que estudia las interacciones supramoleculares ocultas en la estructura y composición química de los materiales. Por lo tanto, la espectroscopia de Raman nos permite comprender la información existente en estos objetos pertenecientes al patrimonio cultural ecuatoriano sin dañarlos o causar lesiones. Esta técnica está permitiendo a los conservadores de arte, restauradores de historia, arqueólogos y arqueometristas descubrir todo tipo de secretos escondidos en obras de arte y antiguos tesoros nacionales. En la espectroscopia Raman, los fotones del láser interactúan con las moléculas y se dispersan. La mayoría de los fotones se dispersan elásticamente, de modo que los fotones emitidos tienen la misma longitud de onda e intensidad que los fotones absorbentes. Algunos de los fotones incidentes se dispersan de forma inelástica, por lo que sus longitudes de onda e intensidades se desplazan. El espectro de luz con longitud de onda desplazada se denomina espectro Raman y cada línea del espectro corresponde a un modo de vibración específico de los enlaces químicos en una molécula. Cada molécula tiene un espectro Raman único y su alta sensibilidad le permite detectar cantidades muy pequeñas de pigmentos orgánicos naturales que han estado ocultos hace mucho tiempo. En este proyecto, nuestro objetivo es analizar y estudiar las estructuras internas y las interacciones moleculares de cuatro vasijas del sitio imperial tardío de Caranqui-Inca por medio de la espectroscopía Raman. Se planea comparar las muestras del estudio con su contraparte parental más cercana en los materiales actuales.

Palabras clave: Espectroscopía Raman, patrimonio cultural, arqueológico, espectro.

Abstract

Raman spectroscopy carved out a niche in the field of diagnostic, analysis and conservation of cultural heritage and different artistic works such as archaeological objects. This archaeometry technique allows us to improve the study of different Ecuadorian ancient cultural heritage and the preservation of the structural properties of these materials. However, a major challenge for researchers is the proper assessment of the provenance and the chemical and structural composition of these individual pieces of cultural heritage due to their lack of archaeological context and advanced characterization techniques. Raman spectroscopy is a non-destructive precise technique that study the hidden supramolecular interactions with the structure and chemical composition of materials. Thus, Raman spectroscopy could potentially allow us to undercover hidden information around the long-term preservation of cultural heritage materials based on their internal composition without damaging the historical samples. This technique is allowing art conservators, restorers of history, archaeologists and archaeometrists discover all sorts of secrets hidden in artworks and ancient national treasures. In Raman spectroscopy, photons from the laser interact with molecules and are scattered. Most photons are elastically scattered so that the emitted photons have the same wavelength and intensity as the absorbing photons. Some of the incident photons are inelastically scattered so their wavelengths and intensities are shifted. The spectrum of wavelength shifted light is called the Raman spectrum and each line in the spectrum corresponds to a specific vibrational mode of the chemical bonds in a molecule. Each molecule has a unique Raman spectrum and its high sensitivity lets detect very small amounts of natural organic pigments which have been hidden long time ago. In this project, we aim to analyze and study the internal structures and molecular interactions of four vessels from the late imperial site of Caranqui-Inca by means of Raman spectroscopy. It is planned to compare the samples of the study to their closest parental counterpart in nowadays materials.

Keywords: Raman spectroscopy, cultural heritage, archaeological, spectrum.

Contents

List of Figures

List of Tables

Chapter 1
Introduction

Throughout the history of humanity civilizations have been born and have died in the passage of time. It's a cycle that catches us all, and in this loop, as human beings we drop objects on those little timelines. As we know, each culture had different types of traditions, within each of these there were creations of different objects that represented tools for their daily lives. A large number of ancient man-made artifacts were made in the form of ceramics, glass, and porcelain. And they have always been an interesting object of scientific study due to the important artistic and anthropological representation that they had in different civilizations. Pottery was considered one of the fundamental bases of the great civilizations, due to this archeology, archaeometry, physics, chemistry and many sectors of science have made so much effort in the study of these ancient objects.

The information obtained from these ancient objects is of vital importance to science. When an ancient object is studied, a deep analysis of the manufacturing process is carried out, the materials that were used, their origin, the use they provided and the environmental conditions that affected its physical and chemical structure. All of this gives us a scientific perspective on the characteristics of a culture. In this way, we can recreate and study certain patterns and behaviors that communes, towns, cities and empires had.

In order to carry out these studies, human beings have had to develop many techniques and with the advancement of technology, these techniques have been modified or developed. Creation is the best quality of humanity and its development allows to perform the advancements. Technology has been the key to being able to grow in many scientific fields, for this reason, the mechanisms to carry out studies of ancient pieces or objects are of fundamental importance.

1.1 The physical science behind the analysis of ancient pottery

Provenance studies

Within the study of cultural heritage there is a detailed process to study the place where artifacts have been produced: provenance studies. This method is used to identify the place of production of a piece, object or artifact belonging to a culture. Provenance studies can be developed by using a macroscopic or typological study and through a scientific technical study. An important fact about these methods is that we cannot generally associate that an artifact comes directly from an area. These techniques provide us with some qualitative and quantitative features of the studied material, but it is very important that they be interpreted correctly. This is due to the fact that the production areas of these materials can be associated with various manufacturing points of some artifacts or object[1].

Provenance studies consist of two major phases:

- Characterization of ceramic, porcelain and glass products.
- Study of local raw materials.

The objects for which it is easier to ascertain the provenance are those having a close connection between raw materials and the finished product. Typically, such studies are undertaken on common pottery, because the production process in that case has been simple, meaning that it has not included excessive and arbitrary modifications of the raw materials[1].

Provenance studies require the joint use of different scientific tools in order to obtain detailed information about the characteristics of certain objects. This is why Raman spectroscopy is used as a materials analysis tool in this work.

1.2 Relationship between the art, archaeology and Spectroscopic Techniques

The relationship that exists between art, archeology and the different techniques of spectroscopy are very close. It is important to know that within spectroscopy there are many techniques for the analysis of matter. Some of these techniques have different characteristics to obtain different results. When we talk about Art and Archeology it is essential to know that we need a spectroscopic technique that allows us to know the history of the material of an object without causing damage.

Dispersive and Fourier transform (FT) Raman microscopy have become established analytical techniques for the identification and study of cultural materials over the past 15 years. Surprisingly, this development has occurred primarily in chemical and materials science departments in academia, rather than in the museum or archaeometry laboratory. Although recently increased interest among conservators, art historians and archaeometrists suggests that this situation may be changing, the widespread acceptance and routine application of Raman microscopy in the fields of art and archaeology have not yet occurred[2].

The absence of Raman microscopy in conservation and archaeometry laboratories is substantially influenced by two factors. First, the instrumentation is expensive, although this financial obstacle can be overcome through strategic budgeting if the desire to incorporate Raman microscopy is sufficient. The second, and perhaps more fundamental, reason is that conservation scientists are generally unfamiliar with the Raman technique and its widespread application in their fields, despite the existence of a large number of publications on the topic[2].

The lack of investigations with Raman microscopy in the conservation field is alarming. Although many articles on the topic have appeared in recent years, only a handful has been published in conservation journals, the balance having appeared in specialist spectroscopy and traditional chemistry publications. Because most of this work originates from chemical science departments in academia, there is pressure on the experimenters to justify their non-traditional research to a somewhat indifferent science community. Moreover, funding for such activities is difficult to obtain from traditional sources in the physical sciences. Therefore, scholars working at the Arts-Science interface are required to defend their work as Science-based rather than Arts-based to both colleagues and funding institutions. This justification is manifested most often by publishing their results in chemical journals that are read and endorsed by the scientists' peers but, unfortunately, not by those in the art. The end result is that, in most instances, the very practitioners who would benefit from it miss a wealth of valuable information. A better record exists for the appearance of Raman microscopy at recent conferences on conservation and archaeometry, but such meetings rarely leave more than a generally inaccessible book of abstracts[2].

Numerous methodologies have been extensively applied in the study of ancient pottery; investigation methods include optical microscopy (OM), scanning electron microscopy (SEM), electron microprobe analysis (EMPA), m-Raman spectroscopy, Fourier transform infrared spectroscopy (FTIR), X-ray diffraction (XRD), high- resolution transmission electron microscopy (TEM), X-ray fluorescence (XRF), particle induced X-ray emission (PIXE), inductively coupled plasma atomic emission spectroscopy (ICP-AES), inductively coupled plasma mass spectrometry (ICP-MS) and other techniques. Among them, (micro) -Raman spectroscopy is now widely applied in the field of cultural heritage, art and archeology[3].

Works on pottery, porcelain and glass, (micro)Raman spectroscopy has been effectively used together with other techniques, mainly XRD, XRF, SEM-EDS, FT-IR and thermal expansion, and more rarely UV-visible reflectance spectroscopy, ion chromatography and electron microprobe analysis[4].

Raman spectroscopy is one of the tools that have generated the most impact in many fields of scientific research. The fields where this technique has a vital impact have been archaeometry and conservation science. And over the years, Raman spectroscopy increases its development and its field of intervention. The development of new methods and data treatment of the spectral information will be a field of continuous research in the field of Cultural Heritage where real samples are always complex mixtures of original and degradations compounds that require new approach to be implemented in the daily practice of Raman spectroscopy[5].

1.3 The importance of Raman Spectroscopy in recent Archeological studies

During the past decade, Raman spectroscopy has been increasingly applied for the analysis of objects of art and antiquities. Since the publication of the database of Raman spectra of pre-1850 pigments the application of this technique in this field has grown exponentially[6]. Although this database and the papers from several groups that appeared around the same time introduced many people to this research field, these were not the first applications of Raman micro spectroscopy in art analysis. In 1979 Dhamelincourt[6] described the coupling of a microscope to a Raman spectrometer and the application to the investigation of artifacts. In general, the first papers focused on instrumental improvements and explored the feasibility of the approach for the investigation of artifacts, centering mainly on pigment identification[6].

The relationship that exists between art, archeology and the different techniques of spectroscopy are very close. The study of the antique paintings is one of the most evident examples of the interaction between scientific analysts, art historians and archaeologists, required not only to understand the problem but also to make optimum use of the harvested data[9]. Although the Raman effect was discovered in the first half of the 20th century, it is only in the 1980's and 1990's that the technique became increasingly accessible for art analysis. This is mainly the consequence of decades of technical improvements, such as the introduction of lasers and charge-coupled device (CCD) detectors, which allowed researchers to expand the range of possible applications[5]. The coupling of spectrometers with microscope optics was an especially favorable evolution, enabling researchers to record Raman spectra of particles down to a diameter of 1 (micro) m - the typical order of magnitude of pigment grains. Additional technical advances, including the introduction of fiber optics Raman spectroscopy, paved the way for new applications of the technique in the cultural heritage field. Overtime, typical uses of Raman spectroscopy evolved from pigment identification (by comparison against a reference database) to more complex cases, such as the study of degradation and corrosion processes, the analysis of organic materials, complex microsamples, etc[5].

Raman Spectroscopy Technique is well-appreciated for its non-destructive character, its small spectral footprint and its ability to record molecular spectra of inorganic as well as organic materials[7]. Among the devices abilities some are significant in these applications, as the opportunity to record spectra at very low laser power which respect sample integrity or the developments of mobile spectrometers. The later seems actually to reach a maturity with at the technical point of view a clear feasibility demonstrated and the treatment of some specific investigations[8]. In general, Raman spectra are typically less complex and have narrower bands compared to infrared spectra[7].

Raman spectroscopy does not produce an alteration or consumption of the sample we are trying to study, allowing to perform further investigation with other techniques, which is a fundamental aspect in the field of cultural heritage, where usually the samples are microscopic and the sampling is often unique. The widespread use of Micro-Raman spectroscopy is due to the possibility to identify minerals of a ceramic sample on the basis of the vibrational Raman spectra in a selected spot, due to its excellent spatial resolution. The possibility to select a well-defined spot in a micrometric range can minimize mistakes and allows identifying single crystals without the interference of the signal of the matrix. Moreover, Micro-Raman technique allows repeating the measure several times in the same spot or in different points of the same sample in a very short time[9].

The application of Raman spectroscopy to the analytical characterization of archaeological materials is now well established although the common occurrence of fluorescence emission backgrounds, which arise from specimen degradation, absorption of impurities from the depositional environment or percolation of materials from the upper parts to the archaeological site is a problem for the analysis of some sample. That is why new improvements and experiences are required to solve such problems and to continue the research in this particular field[8].

In order to study certain ceramics and paintings, it is important to know that they are made of different materials. Over time these materials have changed, there is even a cultural heritage that is made up of materials from different periods. The study of materials and their mixtures are of vital importance in order to understand the result that was materialized in works or objects. For example, Tomasini[9] suggest a characterization by means of Raman spectra of different pigments based on carbon to distinguish between the various kind of carbonaceous materials used in pictorial and archaeological samples. The most antique and well-known pigments, such as hematite and carbon, still require deep studies to understand their sources, preparation methods and their uses in historical and pre-historical times[5].

The analysis of the materials used in ancient artworks must not be limited to the substances intentionally used by the artists, because preservation along the time depends also on the surrounding materials, on the environmental agents and on the man-made alterations they suffer. Thus, the alteration products and the deterioration agents should be identified and studied to fulfill with the complete characterization of all materials present. This cannot be afforded with the use of a single technique and usually a multi-technique approach is required[5].

In Raman spectroscopy, it is essential to understand the materials that are part of the structure of the objects of study. The best way to understand these materials is through the analysis of the information obtained after having carried out the measurement process with a Raman spectrometer. This information gives us the correct ways to understand the history of our object of study.

The analysis using this technique is based on induce a monochromatic beam of light with a certain frequency on a sample where the molecular characteristics are to be determined. When this process is carried out, the objective is to analyze and examine the information of the light scattered by that sample. A large amount of scattered light has the same frequency as incident light, but a very small fraction has a frequency change which is the result of the interaction of light with the matter present in the sample[1, 3]. Part of the light that maintains the same frequency as the incident light does not provide any information about the composition of the sample analyzed. On the other hand, the scattered light that presents frequencies different from the incident radiation, gives us essential information about the molecular composition of the sample and is known as Raman scattering[1]. These frequencies take the name of Raman frequencies and give us the characteristics of the chemical nature and the physical state of the sample, in addition they are independent of the incident radiation. This information is called 'spectrum'. It is important to know that spectra are like fingerprints of molecules, so when we analyze objects with different compounds, we must understand each of these separately. The individual analysis of the molecules that are part of the structure of an object provides us with a frame of reference to be able to affirm or deny its existence[1, 3].

1.4 Review of Raman studies on ancient pottery, porcelain and glass

The first chemical analyzes of artworks and archaeological artefacts were accomplished historically and reported by Rene-Antoine Ferchault de Réaumur in France in a series of publications between 1716 and 1739 and by Sir Humphry Davy in the UK in 1815, respectively: the former appeared in the Memoires Academie de Sciences, Paris, on pottery, glass and porcelains and the latter on wall painting fragments from Pompeii was published in an issue of the Philosophical Transactions of the Royal Society in 1815[10].

Both studies were directed at the identification of the pigments used by ancient artists and in both cases the complete destruction of the specimens was undertaken; Sir Humphry Davy especially commented on this undesirable although necessary aspect of his work from him. Even in 1922, the situation had remained unchanged and Eccles & Rackham in their classic publication on the wet chemical analyzes of English, Welsh, Chinese and Continental porcelains in the Victoria & Albert Museum's collection had to destroy valuable and documentary pieces to achieve their objectives in the determination of the chemical composition of the selected specimens. The application of analytical spectroscopic and diffraction techniques in conjunction with microscopic interrogation to determine the elemental and molecular composition of artworks and archaeological specimens, usually with microsample region interrogation, is now well established and can be accomplished with minimal or no specimen sampling and additionally this can sometimes be performed in situ using portable instrumentation[10].

It was several years before Raman spectroscopy was applied to genuine archaeological materials, when in 1991 the biodeterioration of exposed Renaissance frescoes and later in the same year from bio-deteriorated cave art were reported. Then in 1995, Raman spectroscopic studies of archaeologically excavated biomaterials, specifically the mummified skin of Otzi the Alpine Iceman, dating from 5200 BC, were reported using a sample that would be later destroyed by accelerated mass spectrometry in a radiocarbon dating experiment. Since then the field has advanced rapidly due to a wider selection of excitation wavelengths being made available, especially extension into the near infrared region where the competition of fluorescence emission is minimized, the use of microscopic examination to interrogate microgram and sub microgram quantities of material, the availability of portable, transportable and, more latterly, hand-held instrumentation to effectively bring the laboratory to the specimen, art work or artefact and better detection systems and techniques to enhance the weaker Raman bands over often significant background emission which arises particularly from specimens taken from archaeological excavations and depositional environments[10]. Thus, several advantages of Raman spectroscopy are now manifest for the non- destructive or minimally destructive acquisition of materials identification from art works and archaeological objects which makes it an established technique of choice for researchers at the arts/science interface in association with historical provenance. This has given rise to its usage for 'forensic art' investigations, which are now seen as an essential prerequisite for the establishment of a holistic analytical portfolio of an art work. In this context, Raman spectroscopic data have been involved in several high- profile case studies[10].

The plenitude of material in art and archeology to which Raman spectroscopy has contributed precludes a comprehensive treatment of both areas here[11]. There is a great variety of cultural heritage materials on which studies have been developed. In the world the analysis of materials by means of Raman spectroscopy is very wide.

The production of pottery dates back to the Neolithic/Paleolithic transition (>15,000 B.C. in Japan, Siberia and Africa) and requires heating above 600–650 °C to produce hard and robust artifacts by means of liquid phase sintering[12]. The use of Raman spectroscopy for the characterization of ancient pottery began about 20 years ago, and since then they have mainly focused on the identification of pigments used on ceramics.

Chapter 2

Raman Spectroscopy

2.1 Theorical Background

Raman spectroscopy was developed in 1928 by Sir Chandrasekhara Venkata Raman, hailed by Lord Rutherford as one of the four most important discoveries in physics made up to that time[10]. This magnificent scientist received the Nobel Prize in Physics in 1930. He discovered this phenomenon with the use of basic instrumentation. Raman used sunlight as a source and a telescope as a collector. He used his eyes like two big detectors. It is incredible that a phenomenon as difficult to understand with the naked eye as Raman scattering was discovered in this way. Although initially having several advantages over infrared spectroscopy for molecular characterization, the application of Raman spectroscopy to the analysis of art objects was not forthcoming until the advent of the MOLE (Molecular Optical Laser Examiner) Raman microprobe in 1975 and reports of the determination of pigment composition on manuscripts in museum collections soon followed[10].

Gradually, improvements in the various components of Raman instrumentation took place. Early research was concentrated on the development of better excitation sources. Various lamps of elements were developed (e.g., helium, bismuth, lead, zinc). These proved to be unsatisfactory because of low light intensities. Mercury sources were also developed. An early mercury lamp which had been used for other purposes in 1914 by Kerschbaum was developed. In the 1930s mercury lamps suitable for Raman use were designed. Hibben developed a mercury burner in 1939, and Spedding and Stamm experimented with a cooled version in 1942. Further progress was made by Rank and McCartney in 1948, who studied mercury burners and their backgrounds. Hilger developed a commercial mercury excitation source system for the Raman instrument, which consisted of four lamps surrounding the Raman tube. Welsh introduced a mercury source in 1952, which became known as the Toronto Arc. The lamp consisted of a four-turn helix of Pyrex tubing and was an improvement over the Hilger lamp. Improvements in lamps were made by Ham and Walsh, who described the use of microwave-powered hehum, mercury, sodium, rubidium and potassium lamps. Stammreich also examined the practicality of using helium, argon, rubidium and cesium lamps for colored materials. In 1962 laser sources were developed for use with Raman spectroscopy[13]. Eventually, the $Ar^{+}(351.1 - 514.5nm)$ and the $Kr^{+}(337.4 - 676.4\ nm)$ lasers became available, and more recently the Nd-YAG laser $(1{,}064\ nm)$ has been used for Raman spectroscopy[13].

Progress occurred in the detection systems for Raman measurements. Whereas original measurements were made using photographic plates with the cumbersome development of photographic plates, photoelectric Raman instrumentation was developed after World

War II[13]. Advances in Raman spectroscopy happened over the course of 40 years. The implementation of technology and engineering allowed this technique to develop new tools for sample analysis. In Figure 2.1 we can observe the innovation process that this technique had in the past.

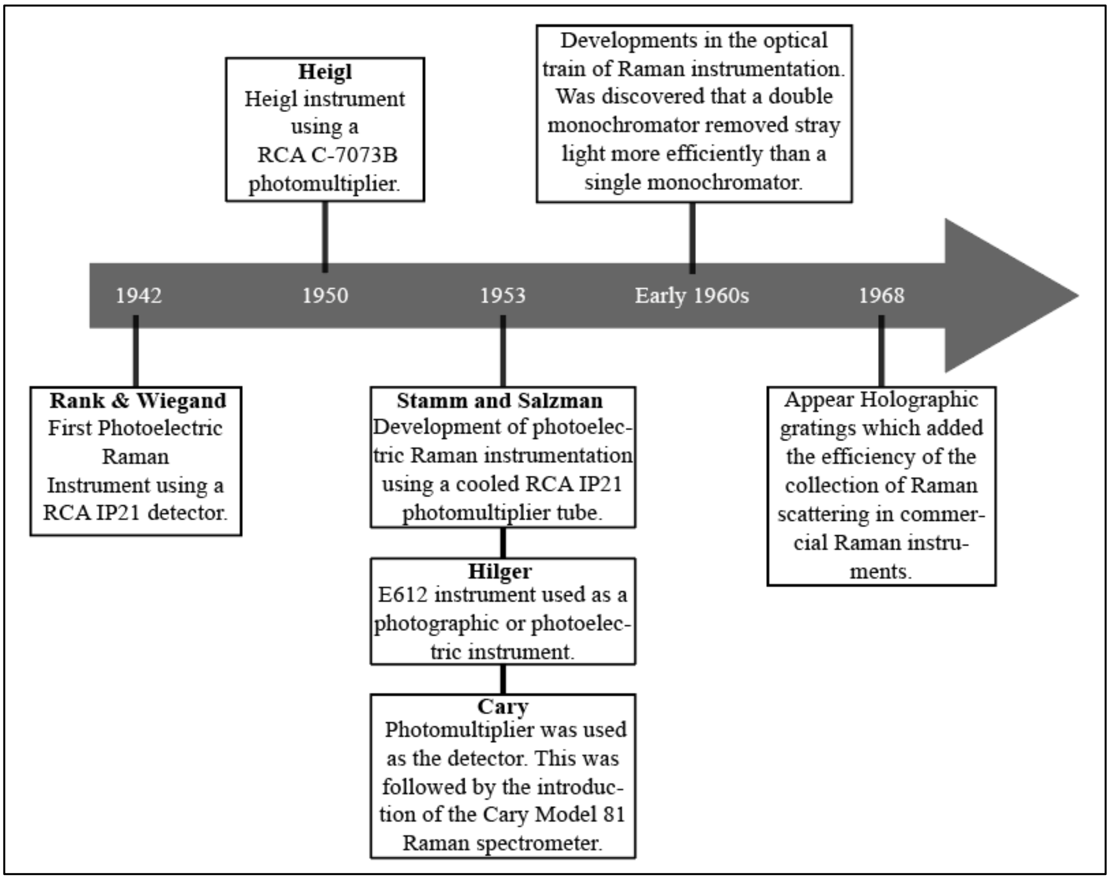

Figure 2.1: Schematic diagram of the history of technological advances of the Raman spectrometer. Image adapted from Ferraro et al. [13]

These developments in Raman instrumentation brought commercial Raman instruments to the present state of the art of Raman measurements. Now, Raman spectra can also be obtained by Fourier transform (FT) spectroscopy. FT-Raman instruments are being sold by all Fourier transform infrared (FT-IR) instrument makers, either as interfaced units to the FT-IR spectrometer or as dedicated FT-Raman instruments[13].

Raman spectroscopy is based on the analysis of inelastically scattered light. Scattering occurs from optical modes of quasiparticles. Classical scatters are optical phonons but other quasiparticles like optical magnons, plasmons or even electronic excitations provide similar sources for the Raman process[14].

Raman spectroscopy probes molecular and crystal lattice vibrations and therefore is sensitive to the composition, bonding, chemical environment, phase, and crystalline structure of the sample material. These characteristics make it an exceptional method for unambiguously identifying materials in any physical form: gases, liquids, solutions, and crystalline or amorphous solids. Raman spectroscopy has thus become an established technique for the study of cultural heritage materials over the past 20 years[4].

2.1.1 Basic principles

Electromagnetic radiation and Molecular Spectra

All light is classified as electromagnetic radiation and consists of alternating electric and magnetic fields and is described classically by a continuous sinusoidal wave like motion of the electric and magnetic fields. Typically, for Raman spectroscopy we will only consider the electric field and neglect the magnetic field component. Figure 2.2 depicts the electric field amplitude of light as a function of time[15].

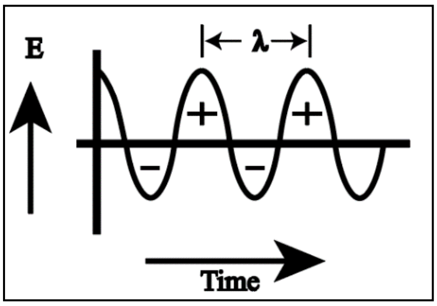

Figure 2.2: The amplitude of the electric vector of electromagnetic radiation as a function of time. The wavelength is the distance between two crests. Image adapted from Larkin et al. [15]

We can use the energy level diagram in Figure 2.3 to explain an absorbance spectrum. The lines labeled E_1 and E_2 represent the ground electronic states and its electronic excited state. Photons of specific energy may be absorbed (or emitted) by a molecule resulting in a transfer of energy. In absorption spectroscopy this will result in raising the energy of molecule from ground to a specific excited state as shown in Figure 2.3[15].

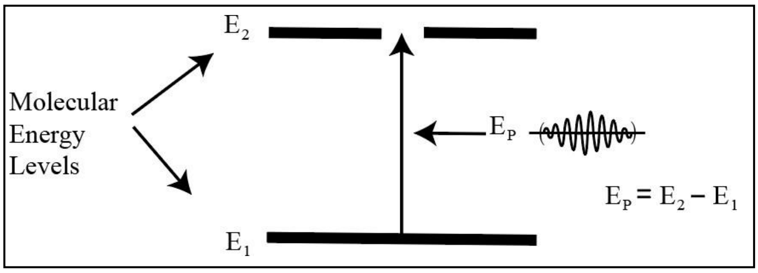

Figure 2.3: Absorption of electromagnetic radiation. Image adapted from Larkin et al. [15]

In Figure 2.4 we can observe a wave of polarized electromagnetic radiation traveling in the z-direction. It consists of the electric component (x-direction) and magnetic component (y-direction), which are perpendicular to each other[13].

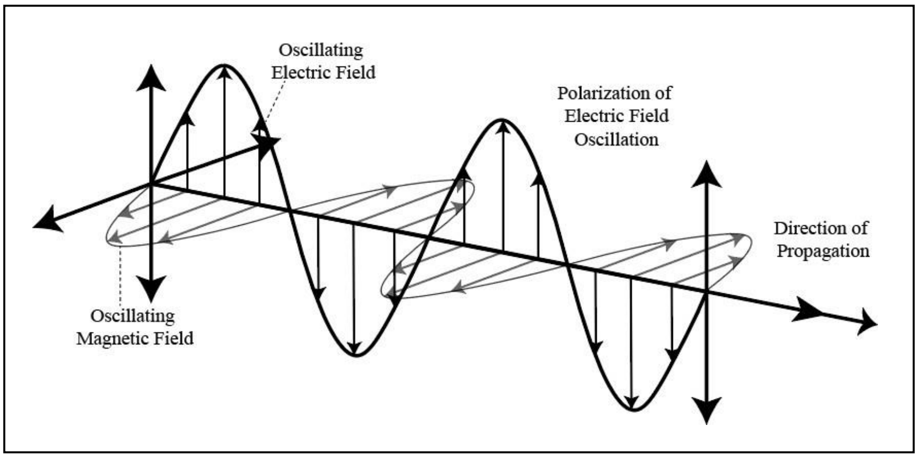

Figure 2.4: Plane-polarized electromagnetic radiation. Image adapted from Larkin et al. [13]

Now, to understand the distances that exist between two points of the same phase in successive waves we need to understand a wavelength, λ, which is measured in Å (angstrom), nm (nanometer) and cm (centimeter)[13]. You can see their relationship below:

$$1\,\text{Å} = 10 - 8cm = 10 - 1nm$$

The frequency, v, is defined as the number of waves in the distance the light travels in one second and c is the speed of light which $3x10^8 m/s$. Therefore:

$$v = \frac{c}{\lambda}$$

In Figure 2.5 we can see the energy units for different sections of the electromagnetic spectrum.

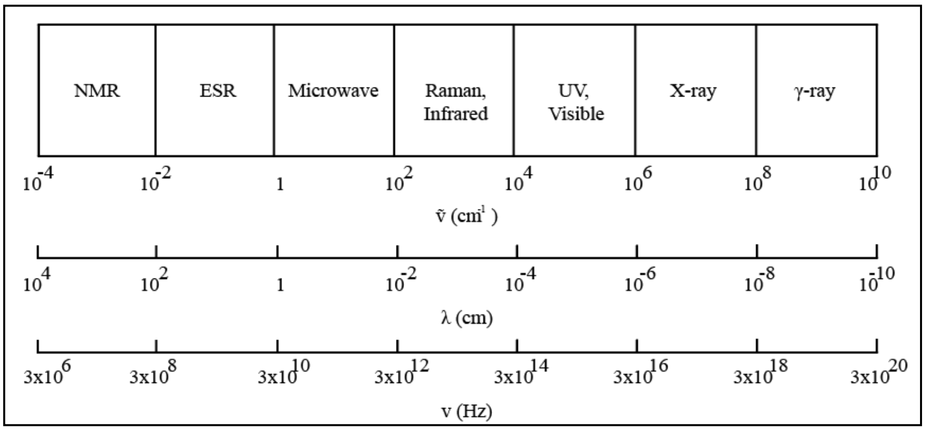

Figure 2.5: Energy units for various portions of electromagnetic spectrum. Image adapted from Larkin et al. [13]

As will be shown later, Raman spectra are intimately related to electronic transitions. Molecular energy levels are more complicated than atomic energy levels because molecules can also vibrate and rotate. The energies associated with such motions lie in different ranges and can therefore be studied separately. Thus, it is important to know the relationship between electronic and vibrational states. On the other hand, vibrational spectra of small molecules in the gaseous state exhibit rotational fine structures. For a collection of molecules, they will be spread out into a large number of rotational and vibrational energy states so any electronic state change (electronic transition) will be accompanied by changes in both rotational and vibrational energies in accordance with the proper selection rules. Thus, any observed electronic transition will consist of a large number of closely spaced members owing to the vibrational and rotational energy changes.

Thus, it is also important to know the relationship between vibrational and rotational states. For complex molecules, these energy changes are difficult to characterize, so we begin with the simple case of a diatomic molecule. For a diatomic molecule the analysis of this motion is relatively straightforward because there is only one mode of vibration, the stretching of the bond. For polyatomic molecules the situation is compounded by the simultaneous motion of many nuclei. The mechanical model employed to analyze this complex motion is one wherein the nuclei are considered to be point masses and the interatomic chemical bonds are viewed as massless springs. To understand the behavior of a diatomic molecule we need to understand its types of transitions. There are three types of energy levels in a diatomic molecule: electronic, vibrational, and rotational. Figure 2.6 illustrates the three types of transitions for a diatomic molecule[13].

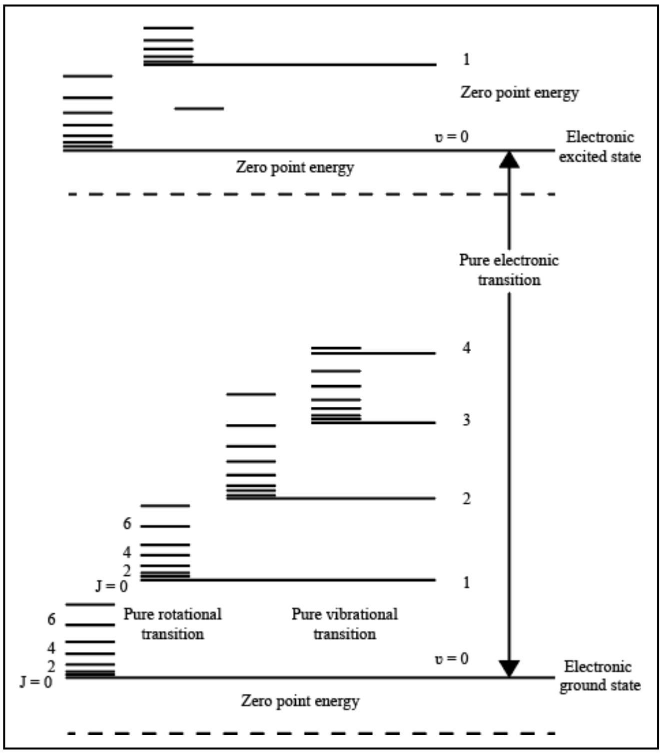

Figure 2.6: Energy levels of a diatomic molecule. (The actual spacings of electronic levels are much larger, and those of rotational levels much smaller, than those shown in the figure.) Image adapted from Larkin et al. [13]

Now, it is important to follow certain steps to understand how these transitions work. In addition, there are certain rules that we must take into account to analyze these behaviors.

Molecular Motion/Degrees of Freedom.

Internal Degrees of Freedom

- **Vibrational Modes**

The movement of the atoms of a molecule when they are under the interaction of a spectroscopic technique is different for each configuration. The molecular motion that results from characteristic vibrations of molecules is described by the internal degrees of freedom resulting in the well-known rule for different vibrations molecules[15]:

For **non-linear** molecules with n atoms, the number of vibrational modes is given by:

$$\mathbf{3n-6}$$

For **linear** molecules, there is one less rotational degree of freedom and the number of vibrational modes is therefore:

$$\mathbf{3n-5}$$

The internal degrees of freedom for a molecule define n as the number of atoms in a molecule and define each atom with 3 degrees of freedom of motion in the X, Y, and Z directions resulting in $3n$ degrees of motional freedom. Here, three of these degrees are translation, while three describe rotations. The remaining $3n-6$ degrees (non-linear molecule) are motions, which change the distance between atoms, or the angle between bonds. Figure 2.7 shows the fundamental vibrations for the simple water (non-linear)[15].

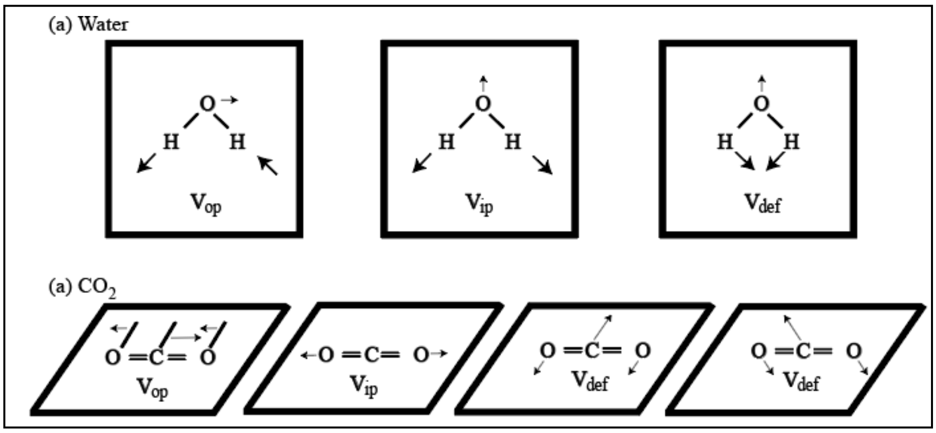

Figure 2.7: Molecular motions which change distance between atoms for water H_2O. Image adapted from Larkin et al. [15]

A simple example of the $3n - 6$ non-linear molecule is water (H_2O) which has $3(3) - 6 = 3$ degrees of freedom. The three vibrations include an in-phase and out-of- phase stretch and a deformation (bending) vibration. Simple examples of 3n-5 linear molecules include H_2, N_2, and O_2 which all have $3(2) - 5 = 1$ degree of freedom. The only vibration for these simple molecules is a simple stretching vibration. The more complicated CO_2 molecule has $3(3) - 5 = 4$ degrees of freedom and therefore four vibrations. The four vibrations include an in phase and out of phase stretch and two mutually perpendicular deformation (bending) vibrations[15].

The molecular vibrations for water and carbon dioxide as shown in Figure 2.7 are the normal mode of vibrations. For these vibrations, the Cartesian displacements of each atom in molecule change periodically with the same frequency and go through equilibrium positions simultaneously. The center of the mass does not move and the molecule does not rotate. Thus, in the case of harmonic oscillator, the Cartesian coordinate displacements of each atom plotted as a function of time is a sinusoidal wave. The relative vibrational amplitudes may differ in either magnitude or direction[15].

Classical Harmonic Oscillator

To better understand the molecular vibrations responsible for the characteristic bands observed in infrared and Raman spectra it is useful to consider a simple model derived from classical mechanics. Figure 8. depicts a diatomic molecule with two masses m_1 and m_2 connected by a massless spring. The displacement of each mass from equilibrium along the spring axis is $X_1$and X_2. The displacement of the two masses as a function of time for a harmonic oscillator varies periodically as a sine (or cosine) function[15].

In the above diatomic system, although each mass oscillates along the axis with different amplitudes, both atoms share the same frequency and both masses go through their equilibrium positions simultaneously[15]. The observed amplitudes are inversely proportional to the mass of the atoms which keeps the center of mass stationary:

$$-\frac{X_1}{X_2} = \frac{m_2}{m_1}$$

The classical vibrational frequency for a diatomic molecule is:

$$v = \frac{1}{2\pi}\sqrt{K(\frac{1}{m_1} + \frac{1}{m_2})}$$

where K is the force constant in dynes/cm and m_1 and m_2 are the masses in grams and v is in cycles per second. This expression is also encountered using the reduced mass where

$$\frac{1}{\mu} = \frac{1}{m_1} + \frac{1}{m_2} \ or \ \mu = \frac{m_1 m_2}{m_1 + m_2}$$

In vibrational spectroscopy wavenumber units, $\bar{v}$ (waves per unit length) are more typically used

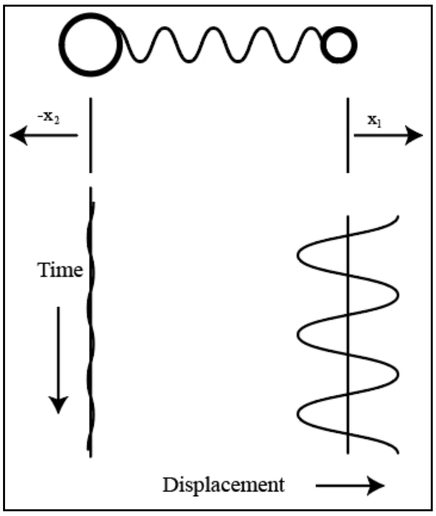

Figure 2.8: Motion of a simple diatomic molecule. The spring constant is K, the masses are $m1$ and $m2$, and $X1$ and $X2$ are the displacement vectors of each mass from equilibrium where the oscillator is assumed to be harmonic. Image adapted from Larkin et al. [15]

$$\bar{v} = \frac{1}{2\pi c}\sqrt{K(\frac{1}{m_1} + \frac{1}{m_2})}$$

where $\bar{v}$ is in waves per centimeter and is sometimes called the frequency in cm^{-1} and c is the speed of light in *cm/s*. If the masses are expressed in unified atomic mass units (u) and the force constant is expressed in millidynes/Ångström then:

$$\bar{v} = 1303\sqrt{K(\frac{1}{m_1} + \frac{1}{m_2})}$$

where $1303 = \left[(\mathrm{Na}x10^5)^{1/2}\right]/2\pi c$ and Na is Avogadro's number $(6.023x10^{23}\mathrm{mole}^{-1})$.

This simple expression shows that the observed frequency of a diatomic oscillator is a function of:

- **a.** **Force constant K**, which is a function of the bond energy of a two-atom bond
- **b.** A**tomic masses of the two atoms** involved in the vibration

Table 1. Approximate Range of Force Constants	
Bond Type	**K (millidynes/Ångstroӧm)**
Single	3-6
Double	10-12
Triple	15-18

Table 2.1: Shows the approximate range of the force constants for single, double, and triple bonds. Values based on Larkin. [15]

Conversely, knowledge of the masses and frequency allows calculation of a diatomic force constant. For larger molecules the nature of the vibration can be quite complex and for more accurate calculations the harmonic oscillator assumption for a diatomic will not be appropriate[15].

Quantum Mechanical Harmonic Oscillator

Vibrational spectroscopy relies heavily on the theoretical insight provided by quantum theory. However, given the numerous excellent texts discussing this topic only a very cursory review is presented here. For a more detailed review of the quantum mechanical principles relevant to vibrational spectroscopy the reader is referred elsewhere[15]. A plot of the potential energy of this diatomic system as a function of the distance, X between the masses, is thus a parabola that is symmetric about the equilibrium internuclear distance, X_e. Here X_e is at the energy minimum and the force constant, K is a measure of the curvature of the potential well near X_e[13,14].

From quantum mechanics we know that molecules can only exist in quantized energy states. Thus, vibrational energy is not continuously variable but rather can only have certain discrete values. Under certain conditions a molecule can transit from one energy state to another ($\Delta v = \pm 1$) and we probe this using spectroscopy. Figure 2.9 shows the vibrational levels in a potential energy diagram for the quantum mechanical harmonic oscillator. In the case of the harmonic potential these states are equidistant and have energy levels E given by[15]:

$$E_i = \left(v_i + \frac{1}{2}\right) h\nu \quad v_i = 0, 1, 2 \ldots$$

Here, ν is the classical vibrational frequency of the oscillator and v is a quantum number which can have only integer values. This can only change by $\Delta v = \pm 1$ in a harmonic oscillator model. The so-called zero-point energy occurs when $v = 0$ where $E = 1/2h\nu$ and this vibrational energy cannot be removed from the molecule[15].

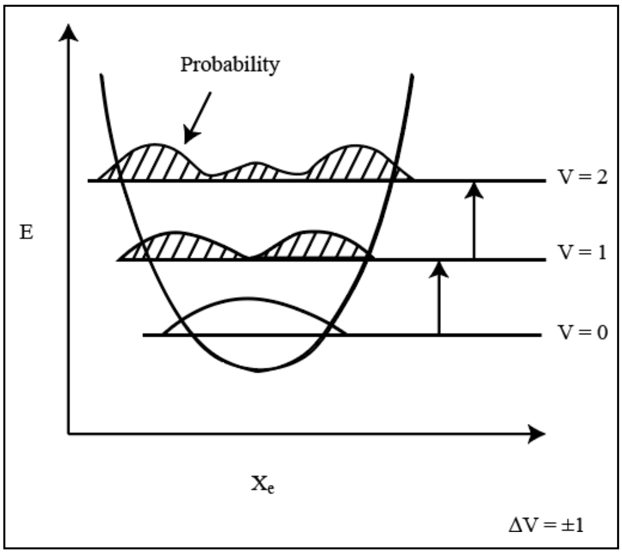

Figure 2.9: Potential energy, E, versus internuclear distance, X, for a diatomic harmonic oscillator. Image adapted from Larkin et al. [15]

Figure 2.9 shows the curved potential wells for a harmonic oscillator with the probability functions for the internuclear distance X, within each energy level. These must be expressed as a probability of finding a particle at a given position since by quantum mechanics we cannot be certain of the position of the mass during the vibration (a consequence of Heisenberg's uncertainty principle)[15].

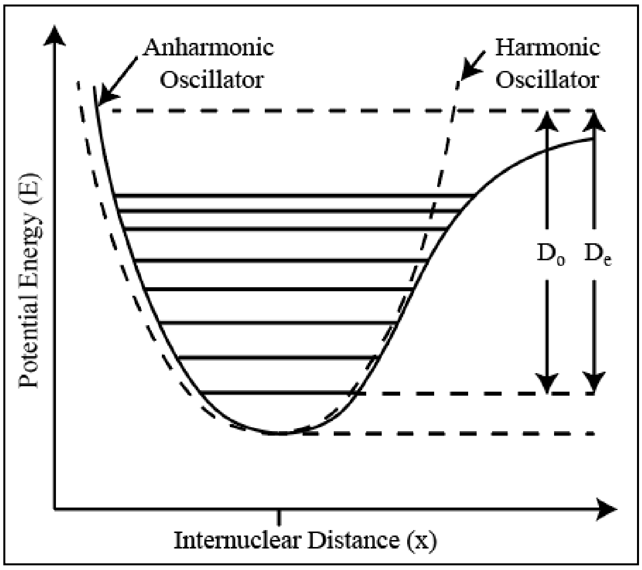

Figure 2.10: The potential energy diagram comparison of the anharmonic and the harmonic oscillator. Transitions originate from the v = 0 level, and Do is the energy necessary to break the bond. Image adapted from Larkin et al. [15]

Although we have only considered a harmonic oscillator, a more realistic approach is to introduce anharmonicity. Anharmonicity results if the change in the dipole moment is not linearly proportional to the nuclear displacement coordinate. Figure 2.10 shows the potential energy level diagram for a diatomic harmonic and anharmonic oscillator. Some of the features introduced by an anharmonic oscillator include the following. The anharmonic oscillator provides a more realistic model where the deviation from harmonic oscillation becomes greater as the vibrational quantum number increases. The separation between adjacent levels becomes smaller at higher vibrational levels until finally the dissociation limit is reached[15]. In the case of the harmonic oscillator only transitions to adjacent levels or so-called fundamental transitions are allowed (i.e., $\Delta v = \pm 1$) while for the anharmonic oscillator, overtones ($\Delta v = \pm 2$) and combination bands can also result. Transitions to higher vibrational states are far less probable than the fundamentals and are of much weaker intensity[13,14]. The energy term corrected for anharmonicity is:

$$E_u = h\nu_e\left(v + \frac{1}{2}\right) - h\chi_e\nu_e\left(v + \frac{1}{2}\right)^2 + \cdots,$$

Where $\chi_e\nu_e$ defines the magnitude of the anharmonicity. Anharmonicity equation shows that the energy levels of the anharmonic oscillator are no longer equidistant, and the separation decreases with increasing v as shown in Figure 2.10.[13]

2.1.2 The Raman Scattering Process

To build the main pillars of the world of Raman spectroscopy we must understand the internal process that exists in this phenomenon. Therefore, it is important to do a deep analysis about the scattering process of Raman spectroscopy.

Light scattering phenomena may be classically described in terms of electromagnetic (EM) radiation produced by oscillating dipoles induced in the molecule by the EM fields of the incident radiation. The light scattered photons include mostly the dominant Rayleigh and the very small amount of Raman scattered light. The induced dipole moment occurs as a result of the molecular polarizability α, where the polarizability is the deformability of the electron cloud about the molecule by an external electric field[15].

In the section a) from the Figure 2.11 we see the response of a non-polar diatomic placed in an oscillating electric field. The field relative to the proton center displaces the electron center. The charged plates of a capacitor, which induces a dipole moment in the polarizable electron cloud, can represent the electric field. Here we represent the static electric field by the plates of a charged capacitor[15]. The negatively charged plate attracts the nuclei, the while the positively charged plate attracts the least tightly bound outer electrons resulting in an induced dipole moment. This induced dipole moment is an off-resonance interaction mediated by an oscillating electric field[13, 15]. Section b) shows the process of attraction of electrons and protons by the plates.

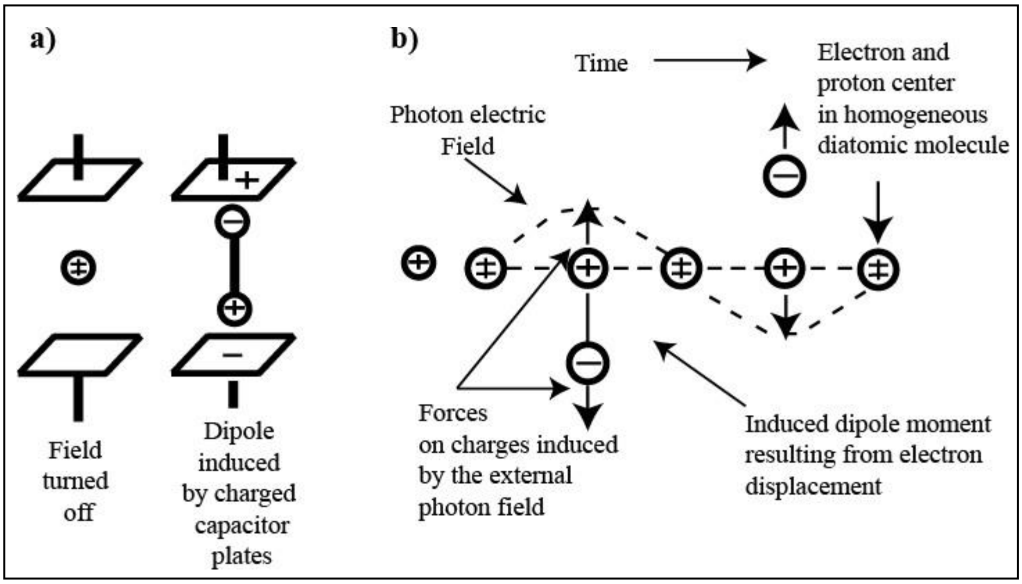

Figure 2.11: Induced dipole moment of a homonuclear diatomic originating from the oscillating electric field of the incident radiation. Image adapted from Larkin et al. [15]

Now, to understand how the generated Raman scattering works, we must understand that in the typical Raman experiment the sample is irradiated by intense laser beams (monochromatic) in the UV-visible region (v_0), and the scattered light is usually observed in the direction perpendicular to the incident beam (Figure 2.12)[13].

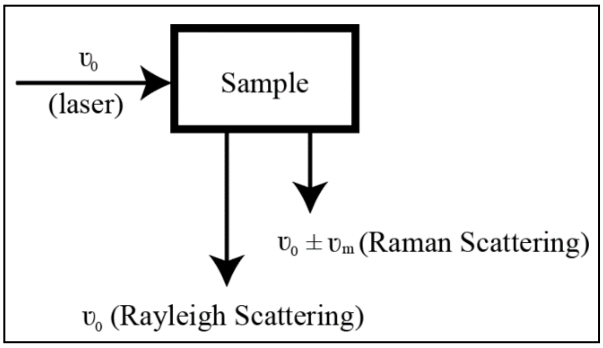

Figure 2.12: Raman scattering process. Image adapted from Ferraro et al.[13]

Laser sources are available for excitation in the UV, visible, and near-IR spectral region ($785\ and\ 1064\ nm$). Thus, if visible excitation is used, the Raman scattered light will also be in the visible region[15]. Then, the scattered light consists of two types: one, called Rayleigh scattering, is strong and has the same frequency as the incident beam (v_0), and the other, called Raman scattering, is very weak (($\sim 10^{-5}$of the incident beam) and has frequencies $v_0 \pm v_m$, where v_m is a vibrational frequency of a molecule[13]. The Rayleigh and Raman processes are depicted in Figure 2.13. In the Figure we can observe that the laser excitation frequency (v_0), is represented by the upward arrows and is much higher in energy than the molecular vibrations. The frequency of the scattered photon (downward arrows) is unchanged in Rayleigh scattering but is of either lower or higher frequency in Raman scattering. The dashed lines indicate the “virtual state” [15].

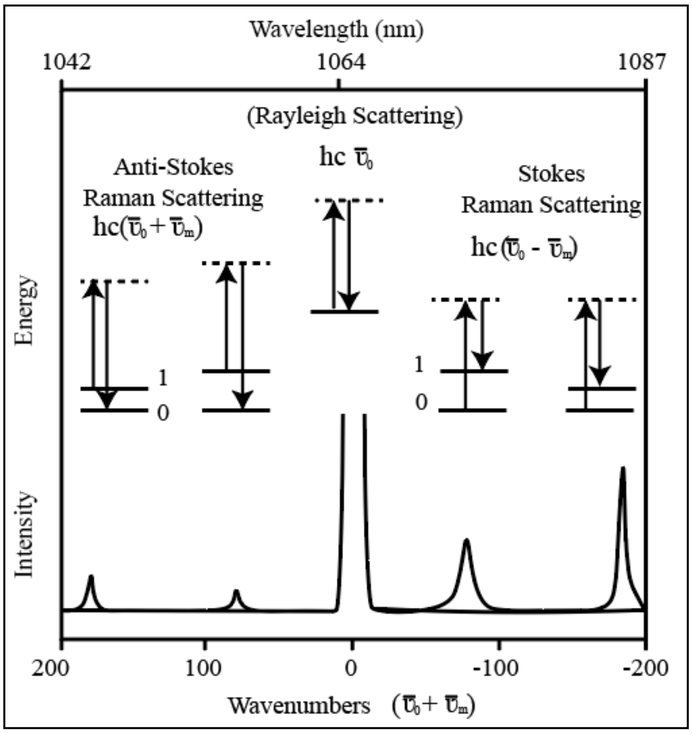

Figure 2.13: Schematic illustration of Rayleigh scattering as well as Stokes and anti-Stokes Raman scattering. Image adapted from Larkin et al. [15]

In Figure 2.13 the $v_0 - v_m$ and $v_0 + v_m$ lines are called the Stokes and anti-Stokes lines, respectively. Thus, in Raman spectroscopy, we measure the vibrational frequency (v_m) as a shift from the incident beam frequency. In contrast to IR spectra, Raman spectra are measured in the UV-visible region where the excitation as well as Raman lines appear[13]

As shown in Figure 2.13 two types of Raman scattering exist: Stokes and anti-Stokes. Molecules initially in the ground vibrational state give rise to Stokes Raman scattering $hc(\overline{v_0} - v_m)$ molecules initially in vibrational excited state give rise to anti-Stokes Raman scattering, $hc(\overline{v_0} + v_m)$ [13]. The intensity ratio of the Stokes relative to the anti-Stokes Raman bands is governed by the absolute temperature of the sample, and the energy difference between the ground and excited vibrational states. At thermal equilibrium Boltzmann’s law describes the ratio of Stokes relative to anti-Stokes Raman lines. The Stokes Raman lines are much more intense than anti-Stokes since at ambient temperature most molecules are found in the ground state[15].

Depending on whether the quasiparticle is absorbed or emitted, the energy of the scattered light is higher or lower than the energy of the incident light. In the first case we speak about anti-Stokes scattering and in the second case about Stokes scattering[14].

This is not necessarily the case for any vibration but rather depends on the mechanical deformation induced in the molecule or in the unit cell of a crystal. The situation can be demonstrated with the model molecules listed in Figure 2.14. The figure shows which deformations Q lead for symmetric diatomic, asymmetric diatomic and symmetric triatomic molecules to a change in the polarizability. In addition, the geometric deformations are indicated which lead to a change of the dipole moment of the molecule. Vibrations of the latter type are infrared active. Column 2 and 3 refer to the change of the polarizability and the dipole moment of diatomic molecules, and column 4 shows the same for three different vibrations of a triatomic molecule. From the symmetry of the vibrations in column 2, 3 and also for the symmetric vibration in column 4 the polarizability is changed by the displacement of the atoms. Therefore, these vibrations lead to a Raman effect and are called Raman active. This is not so for the asymmetric vibrations of the triatomic molecule. In first order the changes induced by one part of the molecule are compensated by the other part[14]. The oscillations are Raman inactive. Similar considerations can be applied with respect to infrared activity. Only the oscillation shown in column 3 and the asymmetric oscillations of column 4 induce a dipole moment and are therefore infrared active. Obviously, a vibration can be either only Raman active or only infrared active or active to both probes. In fact, vibrations can also be inactive or silent to both spectroscopic techniques[14,15].

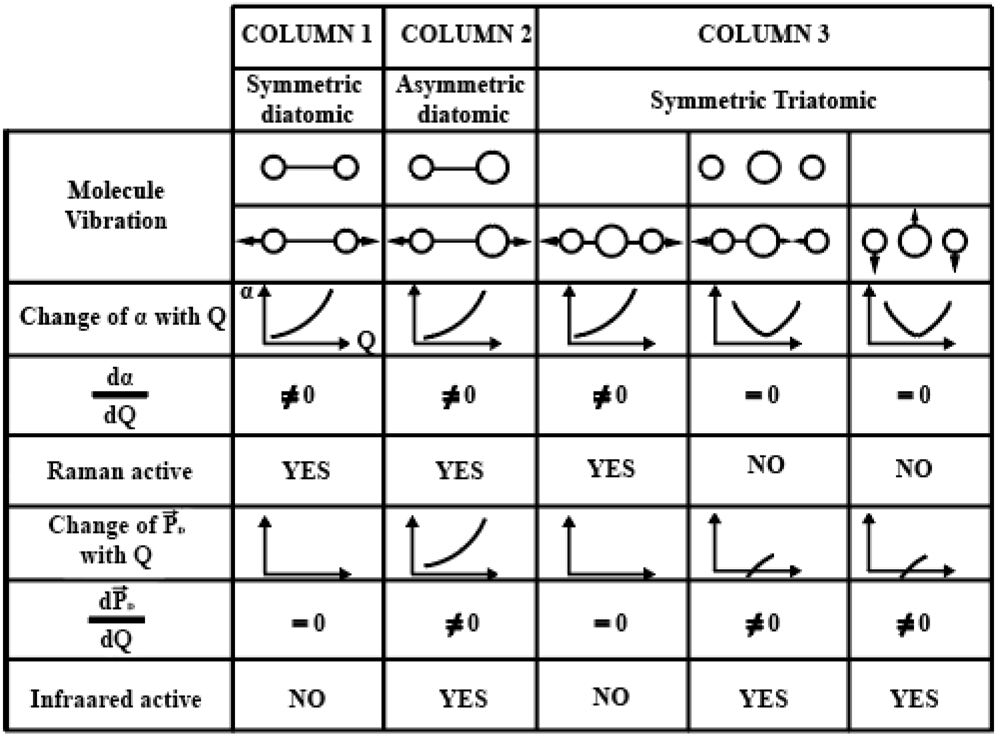

	COLUMN 1	COLUMN 2	COLUMN 3		
	Symmetric diatomic	Asymmetric diatomic	Symmetric Triatomic		
Molecule Vibration					
Change of α with Q					
$\frac{d\alpha}{dQ}$	≠0	≠0	≠0	=0	=0
Raman active	YES	YES	YES	NO	NO
Change of $\vec{P}_o$ with Q					
$\frac{d\vec{P}_o}{dQ}$	=0	≠0	=0	≠0	≠0
Infraared active	NO	YES	NO	YES	YES

Figure 2.14: Selection rules for Raman and for infrared activity of vibrations. Image adapted from Kuzmany et al.[14]

Energy levels for Raman Scattering

Figure 2.15 illustrates Raman scattering in terms of a simple diatomic energy level. In normal Raman spectroscopy, the exciting line (ν_0) is chosen so that its energy is far below the first electronic excited state. The dotted line indicates a "virtual state" to distinguish it from the real excited state. Stokes (S) lines are stronger than the anti-Stokes (A) lines under normal conditions. Since both give the same information, it is customary to measure only the Stokes side of the spectrum[13].

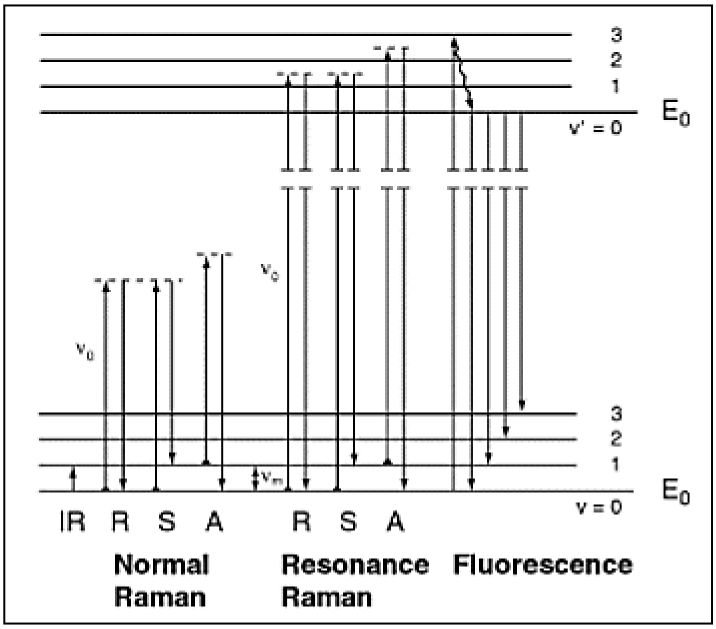

Figure 2.15: Comparison of energy levels for the normal Raman, resonance Raman, and fluorescence spectra. Image adapted from Ferraro et al.[13]

Resonance Raman (RR) scattering occurs when the exciting line is chosen so that its energy intercepts the manifold of an electronic excited state[13]. In the liquid and solid states, vibrational levels are broadened to produce a continuum. *Resonance fluorescence* (RF) occurs when the molecule is excited to a discrete level of the electronic excited state[13]. This has been observed for gaseous molecules such as I_2, Br_2. Finally, *fluorescence* spectra are observed when the excited state molecule decays to the lowest vibrational level via radiationless transitions and then emits radiation, as shown in Figure 2.15 the lifetime of the excited state in RR is very short ($\sim 10^{-14}$s), while those in RF and fluorescence are much longer ($\sim 10^{-8}$ to 10^{-5}s) [13].

Raman Shift

The wavelength of the Raman scattered light depends on the wavelength of the excitation light. This makes the Raman scatter wavelength an impractical number for comparison between spectra measured using different lasers. The Raman scatter position is therefore converted to a Raman shift away from excitation wavelength. Figure 2.16 shows the Raman spectrum of CCl_4[13].

One of the most useful functions in Raman spectroscopy experimentation is the use of the Rayleigh, Stokes and Anti-Stokes Raman Scatter. It is the most important mechanism to calibrate the measurement of our experiment. Calibrating the measurement of our spectrum is one of the most important steps because it helps us to carry out an exact and accurate job. We do this by checking the distances between the Stokes and Anti-stokes wavelengths[13].

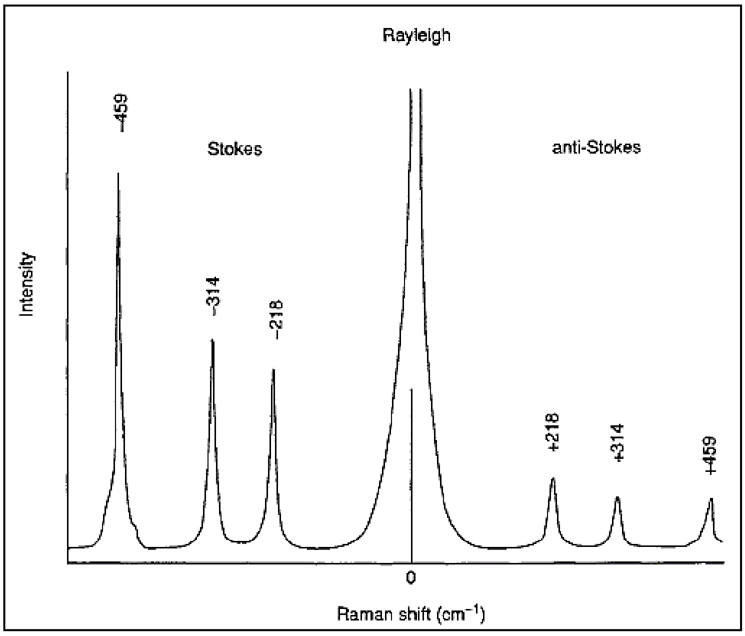

Figure 2.16: Raman spectrum of CCl_4 (488.0 nm excitation). Image adapted from Ferraro et al.[13]

2.1.3 Symmetry: Raman Active Vibrations

Today many sciences are dedicated to studying the atomic structures of molecules for different purposes. We know that in Raman spectroscopy the vibration of molecules is studied, also the structures studies and their reaction behaviors are fundamental part of spectroscopy. All these characteristics are governed by a detailed analysis of their *symmetry*.

The symmetry of a molecule, or the lack of it, will define what vibrations are Raman and IR active. Symmetry may be defined in a nonmathematical sense, where it is associated with beauty—with pleasing proportions or regularity in form, harmonious arrangement, or a regular repetition of certain characteristics (e.g., periodicity). In the mathematical or geometrical definition, symmetry refers to the correspondence of elements on opposite sides of a point, line, or plane, which we call the center, axis, or plane of symmetry (symmetry elements) [13].

In general, symmetric or in-phase vibrations and non-polar groups are most easily studied by Raman while asymmetric or out-of-phase vibrations and polar groups are most easily studied by IR. The classification of a molecule by its symmetry enables understanding of the relationship between the molecular structure and the vibrational spectrum. Symmetry elements include planes of symmetry, axes of symmetry, and a center of symmetry[15].

The number of ways by which symmetry elements can combine constitute a group, and these include the 32 crystallographic point groups when one considers a crystal. Theoretically, an infinite number of point groups can exist, since there are no restrictions on the order of rotational axes of an isolated molecule. However, in a practical sense, few molecules possess rotational axes C_n, where $n > 6$ [13]. Each point group has a character table, and the features of these tables are discussed. The derivation of the selection rules for an isolated molecule is made with these considerations. If symmetry elements are combined with translations, one obtains operations or elements of symmetry that can define the symmetry of space as in a crystal. Two symmetry elements, the screw axis (rotation followed by a translation) and the glide plane (reflection followed by a translation), when added to the five-point group symmetry elements, constitute the seven space symmetry elements. This final set of symmetry elements allows one to determine selection rules for the solid state[13].

Group Theory is the mathematical discipline, which applies symmetry concepts to vibrational spectroscopy and predicts which vibrations will be IR and Raman active. The symmetry elements possessed by the molecule allow it to be classified by a point group and vibrational analysis can be applied to individual molecules[15].

2.1.3.1 Point Symmetry Elements

The spatial arrangement of the atoms in a molecule is called its equilibrium configuration or structure. This configuration is invariant under a certain set of geometric operations called a group. The molecule is oriented in a coordinate system. If by carrying out a certain geometric operation on the original configuration, the molecule is transformed into another configuration that is superimposable on the original (i.e., indistinguishable from it, although its orientation may be changed), the molecule is said to contain a symmetry element[13].

Identity (E)

The symmetry element that transforms the original equilibrium configuration into another one superimposable on the original without change in orientation, in such a manner that each atom goes into itself, is called the identity and is denoted by E or I. In practice, this operation means to leave the molecule unchanged[13].

There are some rules to verify the identity of a molecule:

- It does nothing, has no effect.
- All molecules possess the identity operation.
- E has the same importance as the number 1 does in multiplication and is needed in order to define inverses.

Rotation Axes (C_n)

When a molecule is rotating on an axis of a new configuration that is indistinguishable from the original then the molecule has a rotational axis of symmetry. The rotation can be clockwise or counterclockwise, depending on the molecule. For example, the same configuration is obtained for the water molecule whether one rotates the molecule clockwise or counterclockwise. However, for the ammonia molecule, different configurations are obtained, depending on the direction around which the rotation is performed[13]. The angle of rotation may be:

$$\frac{2\pi}{n} \rightarrow \frac{360°}{n}$$

Where n can be 1, 2, 3, 4, 5, 6, . . ., ∞.
Then, for 2, 3, 4 we have:

$$\mathrm{C}_2 = \frac{2\pi}{2} = 180°\ rotation,$$
$$\mathrm{C}_3 = \frac{2\pi}{3} = 120°\ rotation,$$
$$\mathrm{C}_4 = \frac{2\pi}{4} = 90°\ rotation,$$

The order of the rotational axis is called n, and the notation C_n is used, where C (cyclic) denotes rotation. In cases where several axes of rotation exist, the highest order of rotation is chosen as the principal (z) axis. Linear molecules have an infinite fold axes of symmetry (C_∞) [13].

The order of the rotational axis for a H_2O (water) molecule is $n = 2$. Then, the rotation about the axis is contemplated by $C_2 = 180°$We can see this in Figure 2.17.

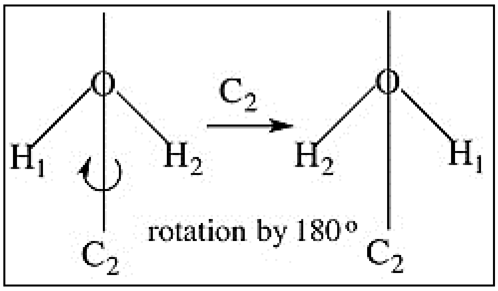

Figure 2.17: Rotational symmetry axis for a H_2O (water) molecule. Image adapted from Ferraro et al.[13]

The selection of the axes in a coordinate system can be confusing. To avoid this, the following rules are used for the selection of the z axis of a molecule:

1. In molecules with only one rotational axis, this axis is taken as the z axis.
2. In molecules where several rotational axes exist, the highest-order axis is selected as the z axis.

3. If a molecule possesses several axes of the highest order, the axis passing through the greatest number of atoms is taken as the z axis.

For the selection of the x axis the following rules can be cited:

1. For a planar molecule where the z axis lies in this plane, the x axis can be selected to be normal to this plane.
2. In a planar molecule where the z axis is chosen to be perpendicular to the plane, the x axis must lie in the plane and is chosen to pass through the largest number of atoms in the molecule.
3. In nonplanar molecules the plane going through the largest number of atoms is located as if it were in the plane of the molecule and rule (1) or (2) is used. For complex molecules where a selection is difficult, one chooses the x and y axes arbitrarily.

Planes of Symmetry (σ)

If a plane divides the equilibrium configuration of a molecule into two parts that are mirror images of each other, then the plane is called a symmetry plane. If a molecule has two such planes, which intersect in a line, this line is an axis of rotation; the molecule is said to have a vertical rotation axis C; and the two planes are referred to as vertical planes of symmetry, denoted by σ_v. Another case involving two planes of symmetry and their intersection arises when a molecule has more than one axis of symmetry.

For example, planes intersecting in an n-fold axis perpendicular to n twofold axes, with each of the planes bisecting the angle between two successive twofold axes, are called diagonal and are denoted by the symbol σ_d. Figure 22. illustrates the symmetry elements of the planar AB_4 molecule (e.g., $PtCl_4^{2-}$ ion). If a plane of symmetry is perpendicular to the principal rotational axis, it is called horizontal and is denoted by σ_h[13].

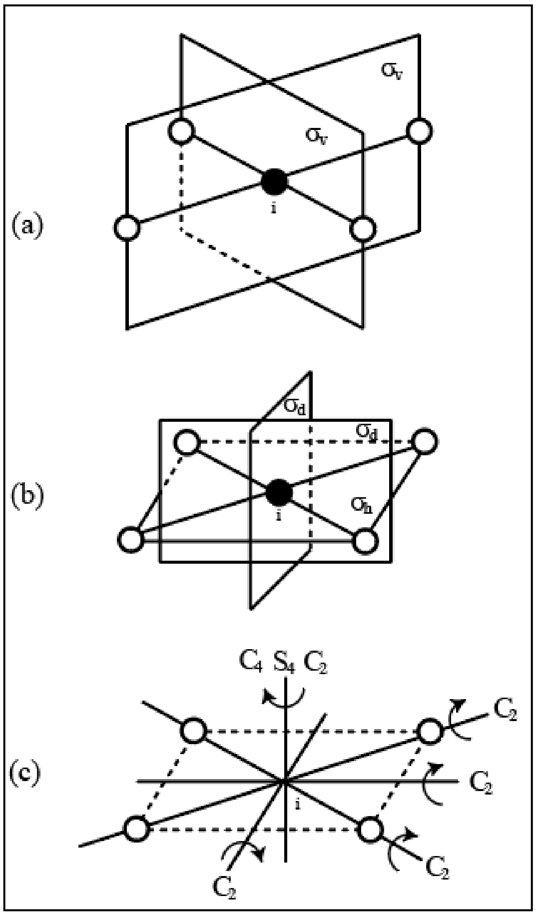

Figure 2.18: Symmetry elements for a planar AB_4 molecule (e.g., $PtCl_4^{2-}$ ion). Image adapted from Ferraro et al.[13]

Center of Symmetry ($\boldsymbol{i}$)

If a straight line drawn from each atom of a molecule through a certain point meets an equivalent atom equidistant from the point, we call the point the center of symmetry of the molecule. The center of symmetry may or may not coincide with the position of an atom[13]. The designation for the center of symmetry, or center of inversion, is i. If the center of symmetry is situated on an atom, the total number of atoms in the molecule is odd. If the center of symmetry is not on an atom, the number of atoms in the molecule is even. Figure 2.18 (c). illustrates a center of symmetry and rotational axes for the planar AB_4 molecule[13].

Rotation Reflection Axes ($\boldsymbol{S_n}$)

If a molecule is rotated 360°/n about an axis and then reflected in a plane perpendicular to the axis, and if the operation produces a configuration indistinguishable from the original one, the molecule has the symmetry element of rotation-reflection, which is designated by S_n[13].

Rules for Classifying Molecules into their Proper Point Group

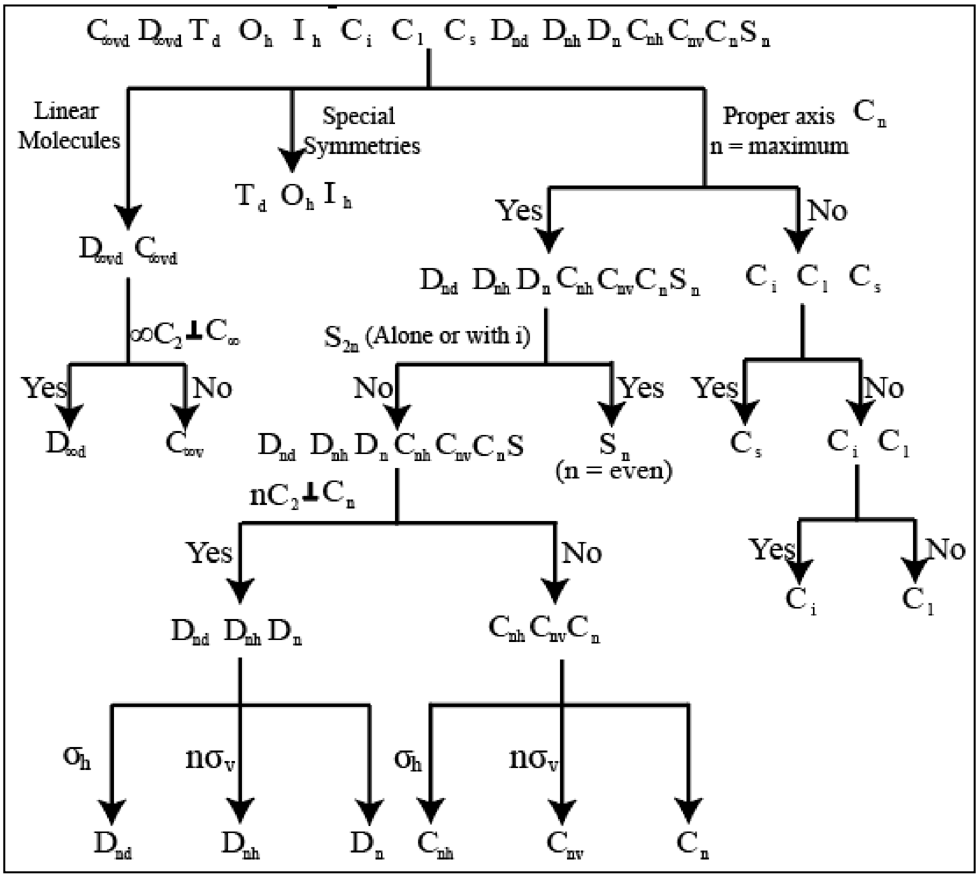

Figure 2.19: Flow Chart of the Method of Classifying Molecules into Point Groups. Image adapted from Zeldin et al.[16]

The method for the classification of molecules into different point groups suggested by Zeldin [16] is outlined in Figure 2.19. The method can be described as follows:

1. Determine whether the molecule belongs to a special group such as $D_{\infty h}$, $C_{\infty v}$, T_d, $O_h\ or\ I_h$. If the molecule is linear, it will be either $D_{\infty h}$ or $C_{\infty v}$. If the molecule has an infinite number of twofold axes perpendicular to the C_∞ axis, it will fall into point group $C_{\infty h}$. If not, it is $C_{\infty v}$.
2. If the molecule is not linear, it may belong to a point group of extremely high symmetry such as T_d, $O_h\ or\ I_h$.
3. If (1) or (2) is not found to be the case, look for a proper axis of rotation of the highest order in the molecule. If none is found, the molecule is of low symmetry, falling into point group C_s, $C_i\ or\ C_l$. The presence in the molecule of a plane of symmetry or an inversion center will distinguish among these point groups.
4. If C_n axes exist, select the one of highest order. If the molecule also has an S_{2n} axis, with or without an inversion center, the point group is S_n.
5. If no S_n exists look for a set of n twofold axes lying perpendicular to the major C_n axis. If no such set is found, the molecule belongs to C_{nh}, $C_{nv}\ or\ C_a$. C_{nv} or C_a. If a σ_h plane exists, the molecule is of C_{nh} symmetry even if other planes of

symmetry are present. If no σ_h plane exists and a σ_v plane is found, the molecule is of C_{nv} symmetry. If no planes exist, it is of C_n symmetry.

6. If in (5) nC_2 axes perpendicular to C_n axes are found, the molecule belongs to the D_{nh}, D_{nd} or D_n point group. These can be differentiated by the presence (or absence) of symmetry planes (σ_h, σ_v, $or\ no\ \sigma$, respectively).

2.1.4 Raman Spectra characteristics of ancient pottery

2.1.4.1 Processing Spectra

Many times, a certain amount of preprocessing is performed on spectral data to make the data more amenable to general processing methods. We will first cover preprocessing and then show how preprocessing is applicable to the more general processing methods. Preprocessing of spectra consists of minor manipulations such as Smoothing, Derivatives, Mean Centering, Normalization, Standard Normal Variance (SNV), Baseline Flattening and Spectral to name a few[13].

Next, we will talk about one of the most used methods in the analysis and data processing of a Raman spectrum: Spectral Subtraction.

Spectral Subtraction

Subtraction is possibly the most used, and often overused, spectral manipulation technique. It is an extremely useful technique because it attempts to obtain spectra of pure components by removing interfering spectral features caused by solvents or other analytes in mixtures. It is also used to remove unwanted background features. Spectral subtraction can be very successful for separating spectra of pure components in the case of mixtures of solid compounds. As long as the various chemical components do not interact and the S/N ratio is good, subtractions can be very successful[13].

One of the most common uses of subtraction techniques is to remove a solvent spectrum from the spectrum of a solution. In most every case there is a solute-solvent interaction, and the spectra of all components in the solution have changed from those of the pure compounds. The changes can occur in band frequencies, intensities, and shapes. The user may gain some insight by performing the subtraction, but the spectra will be distorted[13].

Examples of typical distortions are shown in Figure 2.20 The top spectrum is a mixture of EDTA and water, and the second spectrum is pure water. Two subtractions are shown. The first was based on removal of the water band at 3,245 cm^{-1}; the resulting spectrum is reasonably flat above 2,200 cm^{-1} but contains strong negative bands below 2,000 cm^{-1}. The second result is reasonably flat below 2,200 cm^{-1} but contains the strong water band at ~ 3,245 cm^{-1}. The difficulty is due to the fact that EDTA is hydrogen-bonded to water, so both the water spectrum and the EDTA spectrum have changed in the mixture. This problem is typical of many subtractions. Spectral subtraction can be a very powerful technique for detecting components at low concentrations or those having weak spectral features, but care must be exercised when performing subtractions because the appearance of new or negative bands may not represent the true spectra of the analyte in question[13].

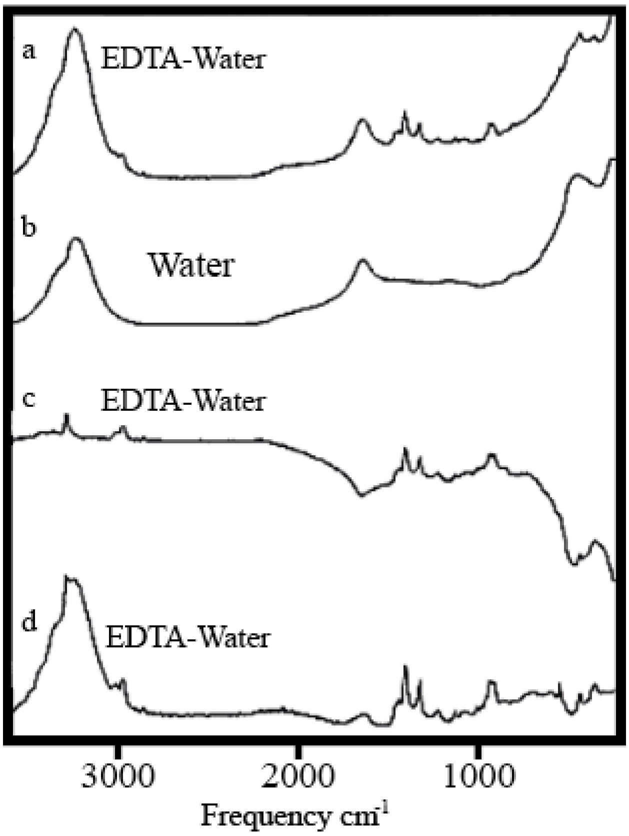

Figure 2.20: Effects of spectral subtraction: (a) Raman spectrum of EDTA-water mixture; (b) Raman spectrum of water; (c) Raman spectrum of EDTA- water minus water; (d) Raman spectrum of EDTA-water minus water. Image adapted from Ferraro et al.[13]

These data processing mechanisms are governed by the analysis of the peaks of the data obtained from the measurement of our sample. These analyzes are usually represented graphically, on the one hand we have the intensity of the scattering of light (y-axis) plotted against the frequency of the light or its wavelength (x-axis). The frequency is measured by the unit of wavelengths that is represented by cm^{-1}[13].

Raman scattering is a fundamental part of sample analysis because it allows us to make measurements of some material that is interacting with a laser in different directions. As we discussed in the previous sections, to identify the chemical and physical composition of a sample, there are three main scattering processes used in Raman spectroscopy: Rayleigh, Stokes Raman and Anti-Stokes Raman[13].

2.1.4.2 Interpretation of Raman spectra

There are a number of approaches which can be used to interpret Raman spectra, the most important are described below:

Identifying functional groups within molecules

The vibrations of certain distinct subunits of a molecule, called its functional groups, will appear in a Raman spectrum at characteristic Raman shifts. Such a shift is similar for all molecules containing the same functional group. These signals are particularly useful when monitoring reactions which involve these functional groups (oxidation, polymerization, etc.), since they provide a direct measure of the progress during the reaction. Using these characteristic shifts makes it possible to relate the spectrum of an unknown compound to a class of substances, as we saw in Figure 2.20[13].

Using the characteristic "fingerprint region"

Apart from the molecular vibrations of specific functional groups, vibrations of the molecular scaffolding (skeletal vibrations) can be detected in a Raman spectrum. Skeletal vibrations are usually found at Raman shifts below $1500\ cm^{-1}$ and have a substance-specific, characteristic pattern. This region, often referred to as the “fingerprint” region of a substance, is the most important part of the spectrum for identification purposes[13].

2.1.4.3 Analysis of the Raman spectrum of ancient ceramics

The spectra obtained by a Raman technique give us the vibrational information of the molecules of different compounds. It is very important to know the spectra that have been obtained in similar studies in order to have a frame of reference about the elements we are studying.

Around the world there are many studies with the Raman spectroscopic technique. The study of ancient ceramics has been studied by these techniques. There are differences in the studies carried out in different areas, even in the same country. This occurs because the elements analyzed may be constituted with a different molecular structure. Therefore, it is essential to take into account similar studies to carry out this work.

The studies that will be shown below were carried out in different parts of the world. The different techniques used to carry out the respective analysis and the spectra obtained will be shown:

MAGNETITE, RUTILE: Micro–Raman spectroscopy investigation on pre-Columbian pottery fragments from Cuanalan (a formative village in the valley of Teotihuacan, central Mexico)[17]. The Raman spectra obtained show that these samples are characterized by the highly heterogeneous body matrix mineralogy due to the presence of a large variety of minerals such as feldspars (alkali polymorph and plagioclase), diopside, magnetite and Timagnetite, and one titanium oxide, rutile[17].

Figure 2.21 shows the Raman spectrum of magnetite $(665cm^{-1})$, Ti-magnetite (cm^{-1}), and rutile $(445cm^{-1} - 607cm^{-1})$. Figure 2.21 (curve (a)) shows an example of a magnetite spectrum acquired in some inclusions which have been found in ceramic materials. The internal vibration of the $Fe^{3+}O_6$ octahedron has been assigned as the major contributor to the main Raman broadband of magnetite detecting around $662– 665\ cm^{-1}$ which is typical of the inverse spinel structures. It is very important to stress that some Raman spectra of magnetite are characterized by a main peak that shifts toward high wave numbers $(670– 675\ cm^{-1})$. This phenomenon occurs because there is the solid solution in the magnetite-ulvöspinel structures where the vibrations of $Ti^{4+}O_6$ and $Fe^{3+}O_6$ octahedra control their Raman spectra features (curve (b)). When forming Ti- magnetite, the main Raman peak is shifted upward, consistent with the increase of $Ti^{4+}O_6$ fractions in their structures. The Raman spectrum of rutile is also shown in Figure 2.21 (curve c), and it agrees well with previously published spectra which exhibit two prominent bands (typical doublet) of 445 and 607 cm^{-1}[17]. Anatase and rutile are common constituents of many soils, sediments, and clays and their identification can provide geological information about the clay sources[18].

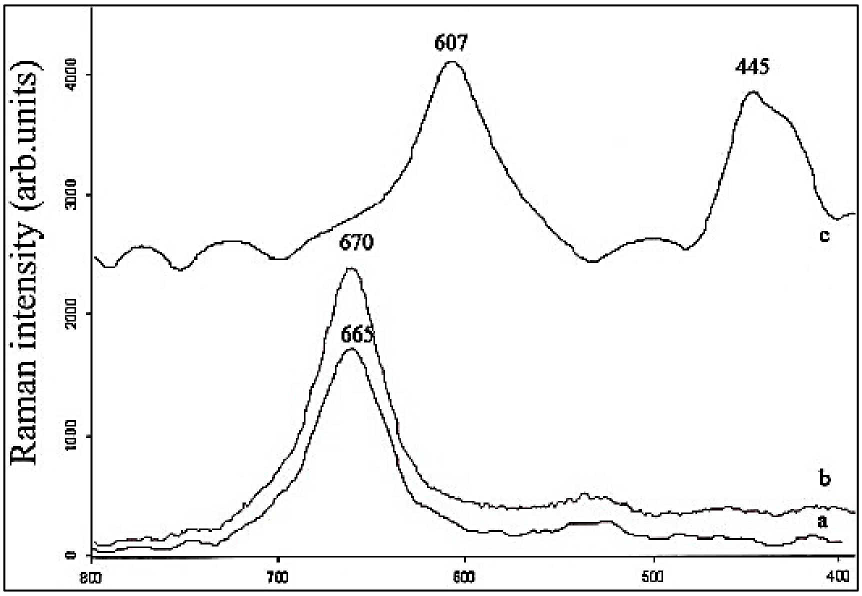

Figure 2.21 Raman spectra of magnetite (curve a), Ti-magnetite (curve b), and rutile (curve c). Note the major peak position shift (665 to 670 cm^{-1}) as a function of magnetite chemistry that is caused by the substitutional solid solution among Fe and Ti. Image adapted from Clark et al.[17]

HEMATITE, MAGNETITE, GOETHITE: The chemical species involved in the present investigation are goethite, hematite and magnetite[19]. Red and yellow pigments are typically associated with iron-oxide related minerals, specifically, hematite and goethite[20]. These compounds are easily differentiated by their Raman spectra (Figure 27), what allows the following of spectral changes with temperature[19].

Reports dating from Roman times indicate that a variety of different shades of yellow and red could be obtained simply heating goethite (α-FeOOH) [19]. Goethite (a yellow compound) turns into hematite (α-Fe_2O_3), which is red, at relatively low temperatures (ca. 260–280 °C), due to a dehydration process[19].

It is well known that, under heating, goethite dehydrates forming hematite, which has been shown to be initially formed as micro or nano domains. These domains coalesce at higher temperatures leading to a more crystalline compound[20]. When a goethite sample is heated (200–1000 8C range) its colour changes to orange, red and dark red. The Raman spectra (ex situ) were obtained for samples heated at 250, 500, 750, 900 and 1000 8C and are shown in Figure 2.22 [19].

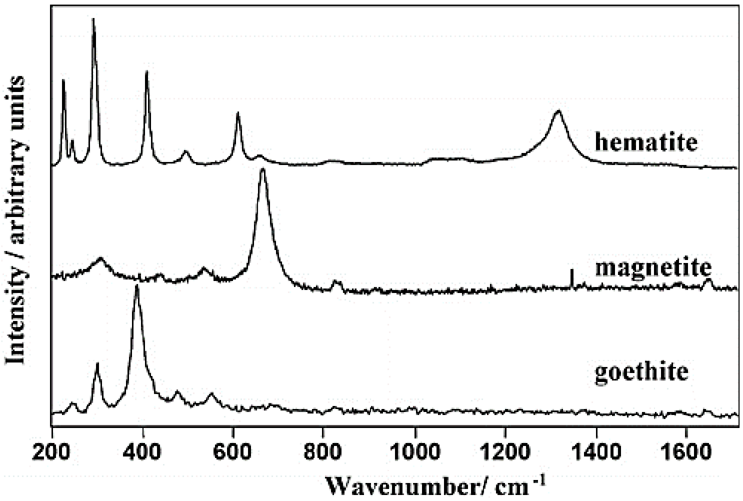

Figure 2.22: Raman spectrum of goethite, hematite and magnetite obtained at room temperatures. Image adapted from Faria et al. [19]

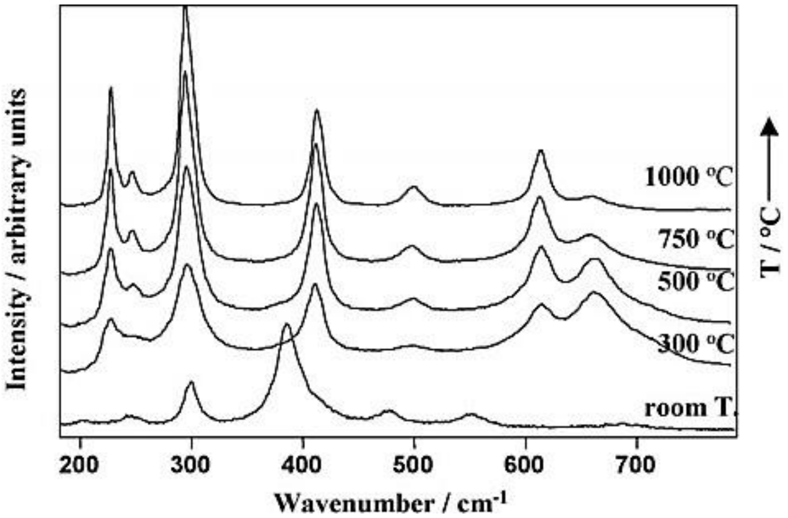

Figure 2.23: Ex situ Raman spectrum of goethite, heated at the indicated temperatures. Image adapted from Faria et al. [19]

CLAYS: Raman spectra of the white pigments (hyena dung, bone white, heated ostrich egg shell, raptor faces and white clay) are shown in Figure 2.24 Four distinct peaks in the spectrum of the white clay/kaolin are OH vibrations that appear between 3500 and 3700cm^{-1}[21]. The bands below 1000 cm^{-1} overlaps with many other bands such as quartz and might be difficult to assign to a specific clay and it should be noted that not all clays will have exactly the same spectrum[21].

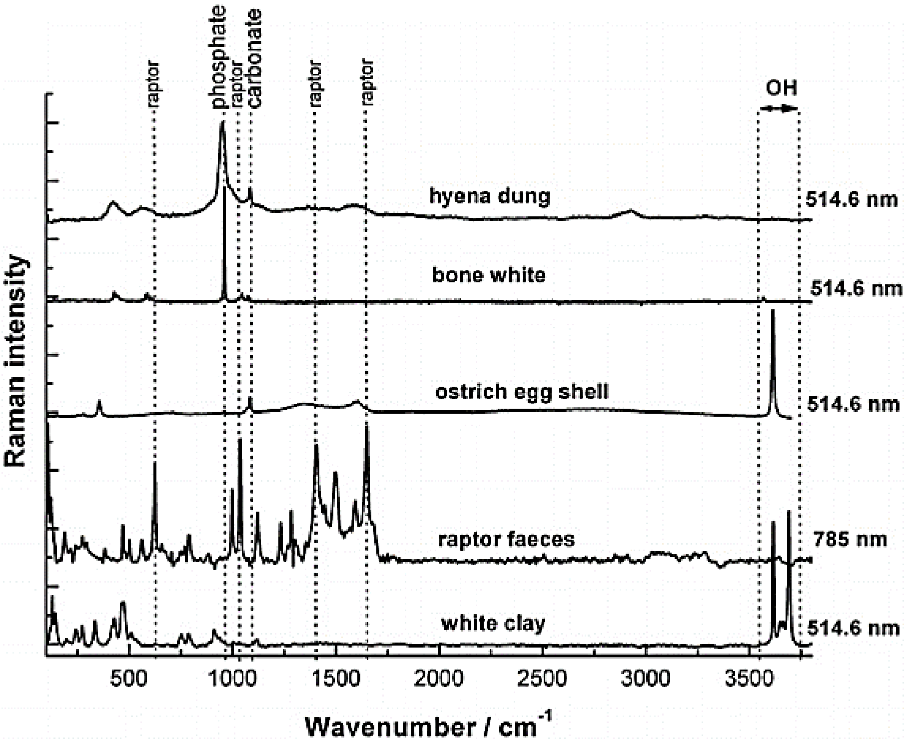

Figure 2.24: Raman spectra of white pigments. White Clay spectra (514.6 nm). Image adapted from Prinsloo et al. [21]

ANATASE: In Figure 2.25 we can see Raman bands (w, weak; m, medium; s, strong; v, very; br, broad) of Anatase (at 143vs, 195vw, 395wm, 514w and 638 m cm^{-1}, Figure 2.25 (a), (b)) [18]. Anatase is one of the three mineral forms of titanium oxide, TiO_2[23]. Anatase and rutile are common constituents of many soils, sediments, and clays and their identification can provide geological information about the clay sources[18]. Anatase transforms irreversibly to rutile in air at about 600 °C, but when it is associated to clay materials, the transformation temperature between the two titanium dioxide forms (anatase to rutile) increases up to 1100 °C. As a consequence, the presence of anatase and the absence of rutile by themselves are not enough to confirm that these ceramics have been manufactured by a cold-working technique[18].

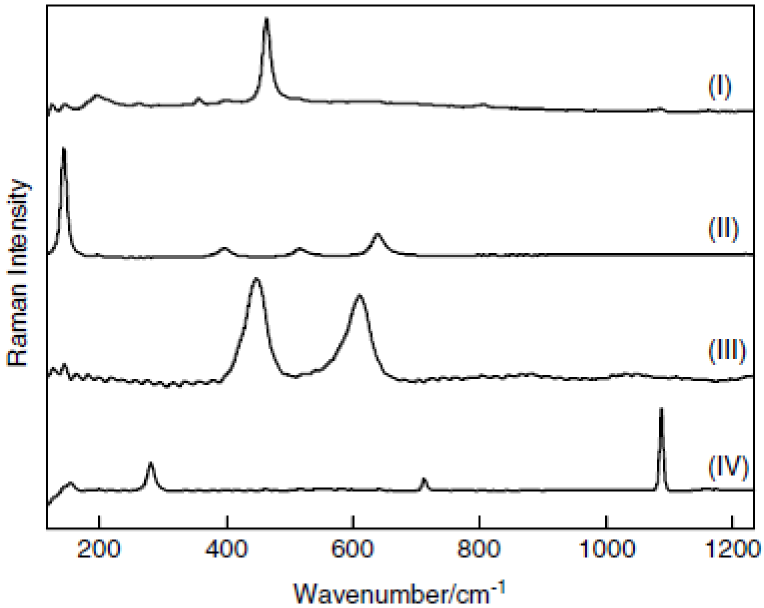

Figure 2.25: Raman spectra of (I) α-quartz, (II) anatase, (III) rutile, (IV) calcite. Source excitation: 785 nm. Image adapted from Sendova et al. [23]

2.2 Raman studies on ancient Ecuadorian pottery

Around the world there are many investigations of ancient ceramics with spectroscopic mechanisms. Raman spectroscopy is one of the most widely used techniques to perform these analyzes. Thanks to the advancement of technology, the use of these techniques has been improving to carry out higher quality studies and research.

In Ecuador, the use of Raman spectroscopy is a new process that is in great demand due to the lack of studies that have been carried out with this technique. Within Ecuadorian archeology there is a deficiency in the use of Raman spectroscopy. Due to this, the only study of ancient Ecuadorian pottery carried out with Raman spectroscopy in Ecuador is presented in this section.

2.2.1 An Archaeometry Characterization of Ecuadorian Pottery

This research is focused on the Jama-Coaque culture, which produced fascinating anthropomorphic and zoomorphic pottery from ca. 240 B.C. until the Spanish Conquest of 1532 A.D. in the coastal region of Ecuador[20]. All these pieces are part of the collection of the Museum of Pre-Columbian Art Casa del Alabado in Quito, Ecuador[20].

In the case of Ecuador, however, most of the pottery available stems from site looting. The lack of an exact determination of their archaeological sites and geological context poses a challenge for modelling the evolution of these cultures in a conclusive manner and determining the provenance of these pieces. Studies of the geological sites provide one way to access this information5. Another way is to study the structural and chemical properties of ceramics and other artifacts - also referred to as archaeometry research. The quality and preservation of pigments in their ceramics, textiles and paintings is a signature of their level of technology. Recent advances in non-invasive instrumentation have opened a window on these ancient potter's choices of materials, mastery of their processing and application, and the society in which they lived[20].

Using a combination of microscopic and spectroscopic techniques, i.e., transmission electron microscopy (TEM), Raman spectroscopy, Fourier transform infrared spectroscopy (FTIR), energy-dispersive x-ray spectroscopy (EDX), and scanning electron microscopy (SEM); the characterizations of some pieces of this culture were developed[20].

For the ceramic characterization process, spectroscopic and microscopic techniques were used from the Jama-Coaque culture of Ecuador (240 B.C. to 1532A.D.) Which occupied 250 km of coastline between the Bahía de Caráquez and the Cabo de San Francisco (Figure 2.26) [20].

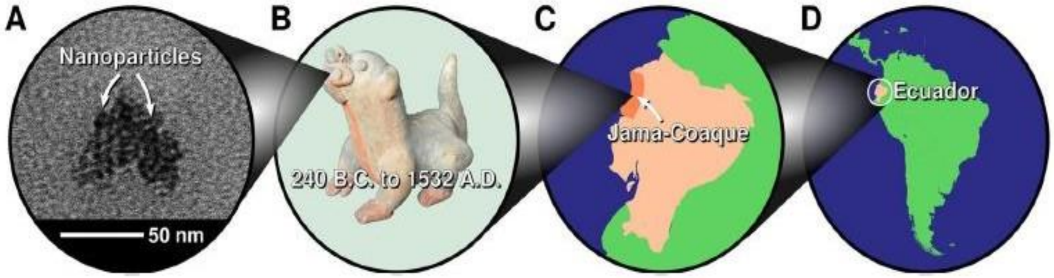

Figure 2.26: (A) TEM micrograph of nanoparticles present in (B) pigment on pottery from (C) the Jama-Coaque culture of (D) South America. Image adapted from Sánchez et al. [20]

The pigments of these ancient pottery have been investigated all over the world since they represent a fundamental part of the identification of different substances of the representative cultures of each country. Laos pigments, as well as the material used for their manufacture are analyzed in detail in this work.

2.2.1.1 Raman Techniques

Figure 2.27 displays photographs of three samples of the Jama-Coaque collection we investigated, designated hereafter as samples A, B, and C. Below each photograph, the palette of colours investigated for each sample is displayed for reference[20].

Figure 2.27: Selected Jama-Coaque pottery samples (A–C) with colour palettes. All photographs are displayed with a similar scale and a palette showing all sampled colours. Image adapted from Sánchez et al. [20]

One of the disadvantages that they had in the analysis by means of Raman is the original location of the sites of the pieces. Figure 2.28 shows selected typical Raman spectra for the pigmented areas obtained from the Jama-Coaque pieces of Figure 2.27, with the positions of the main vibrational modes provided in Table 3. In the red pigments of samples, A and C we identified the presence of iron oxide in the hematite phase, $\alpha - Fe_2O_3$. In a similar way, the yellow pigment of sample A exhibits a very intense band in its Raman spectrum at 398 cm^{-1}, corresponding to the goethite phase of iron oxide, $\alpha - FeOOH$[20]. Notice that other broad peaks that can be related to heat treatment and a potential phase transformation as a function of the temperature, as reported previously. In the black pigment of sample, A recognize typical carbon-related features. In this case, the sp^3 (D band) is slightly stronger than in carbon black, suggesting a higher density of defects. The green pigment of sample A exhibits very intense bands at 1352, 1465, and 1539 cm^{-1} which they assign to copper phthalocyanine. On samples of bare clay for sample A, it was found two broad peaks at 327 and 388 cm^{-1}, which are typical features of heat-treated clay[20]. However, a similar Raman spectrum is observed for the white pigment of sample A, the green and blue pigments of sample B, and the green of sample C, indicating these extracted samples were mainly composed of clay[20].

Sample	Raman (cm^{-1})	Assignment
Black	1350, 1585, 2700, 2900	Carbon Black[a,b,c]
Yellow	230, 398, 470, 540	Goethite[d]
Red	290, 550, 605, 670, 1315	Hematite[e]
Green	606, 694, 850, 1155, 1352, 1465, 1539	CuPc[e]
Clay	327, 388, 482, 548, 603	Clay[f]

Table 2.2: Raman vibrational modes from Figure 2.28 and their assignments[20].

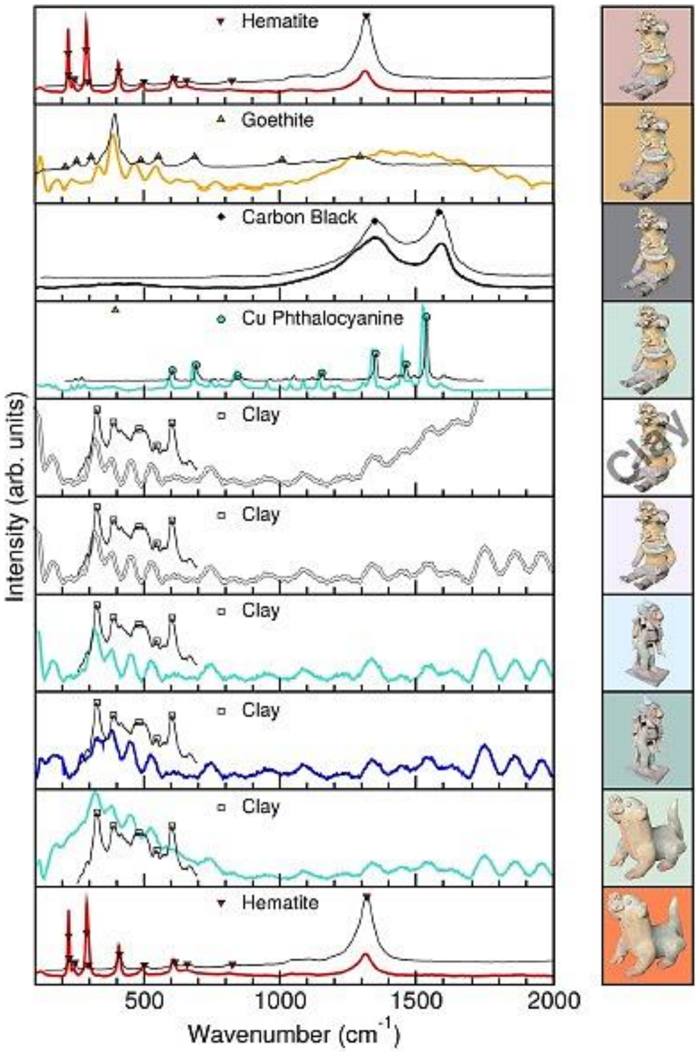

Figure 2.28: Raman spectra (λexc = 633nm) for selected pigments present in Jama-Coaque ceramics (thick lines). Reference spectra (thin lines) and selected peaks for clay (squares), copper phthalocyanine (circles), goethite (triangle up), hematite (triangle down), and carbon black (diamond) are provided for comparison. The sample and colour as background are provided to the right of each spectra. Image adapted from Sánchez et al. [20]

The work was carried out successfully to analyze the 3 ceramic archaeological pieces from Jama-Coaque. Raman spectroscopy is a very important tool for studying materials. Because they are archaeological pieces, this technique is convenient because it does not damage the samples[20].

Chapter 3
Motivation

The passage of the years gives the necessary tools to great cities and empires to make great advances in history, but time is jealous, and the fingerprint of our life lapse needs to be dusted off. History allows us to reconstruct all kinds of things. From scientific advances to anthropological behaviors of ancient communities. The study of ancient pottery is a method to understand the life left by our ancestors.

Raman spectroscopy gives us the opportunity to understand this story, to reconstruct the life of the past. This technique is very important for the development of countries, it is one of the mechanisms that can contribute the most to the study of antiquities. But Raman spectroscopy serves many other functions, spectrometers are capable of analyzing matter, so they have many functions within scientific research.

Research with Raman spectroscopy has a short trajectory in Ecuador. The first Raman spectrometer and the oldest in Ecuador is at the "Escuela Politécnica del Ecuador". It has a life of five years and is part of a spectroscopy laboratory at the university. Unfortunately, there are no archaeological studies with this spectrometer. Because of this, it is about creating new mechanisms to encourage the study of archaeological and artistic pieces by means of Raman spectroscopy. The second Raman spectrometer in Ecuador is located at the "Yachay Tech" university. Thanks to this spectrometer this work was developed. It is important to say that the instruments and tools that universities provide us allow us to grow as researchers and promote the development of science in the country.

The lack of studies of Raman spectroscopy on the cultural heritage of ancient civilizations in Ecuador provides us a wide margin of analysis and research. It is our duty as curious humans to rescue the history that is buried in Ecuador. As an Ecuadorian, I am very pleased to develop studies about our culture and try to reinforce the history we have about our past. The identity of the human being and cultures is a factor of vital importance.

One of the most important settlements in our history was the Caranqui country. The Caranqui Culture is one of the last native settlements before the Pre-Hispanic Period in Northern Ecuador. The development of this country was performed by the creation of different structures of anthropological architecture. These architectural buildings had different purposes and objectives in the structure of the country. One of the most important buildings were the *tolas*. Based on both archaeological investigation and ethnohistoric accounts, these impressive structures likely represent platforms for elite or chiefly residences and served as foci of ritual and commercial activities. The importance of the *tolas* in this investigation is due to the number of vessels that have been collected in their surroundings, and also allows us to reaffirm the value that these sacred areas had for the inhabitants and foreigners of Caranqui[24, 25].

In the Caranqui country there were large pot manufacturing centers. This is due to the knowledge that existed about the handling of different materials. In the process of fighting for control of the territory between Caranqui and the Incas, there were large settlements of potters in these areas. Understanding the processes of manufacture and use of ancient pottery provides us with vital information to understand and reestablish anthropological behaviors of these cultures.

The history of many events that occurred in the Caranqui country are buried. It is very important that studies and research are carried out to know the history that precedes us. Raman spectroscopy allows us to analyze in detail the composition of the materials that were used to create all kinds of objects made of clay. This technique is a tool that benefits the study of many scientific aspects of ancient peoples. Due to the great importance that the tolas had in the cultures of Caranqui and different countries in Ecuador, I am interested in developing Raman spectroscopy studies of vessels found in the vicinity of these tolas. It is essential that the development of spectroscopy techniques be used to analyze data about the ancient cultures that inhabited Ecuador. Through these techniques essential information can be obtained to understand the identity, worldview and traditions of our ancestors.

General and Specific Objectives

General Objective:

Analyzing the four vessels from Caranqui zones allows us to have very important information about the composition of the materials with which they were made. The data obtained will guide us precisely to the discernment of the compounds and elements that have been used, under what conditions they were manufactured and the locations of the vessels for their manufacture and final use. Collecting all this information gives us an opening in the contribution to the investigation of the inheritances of the ancestral communities. Creating anthropological and archaeological study mechanisms, through spectroscopy techniques in physics, favors the development of knowledge about our footprint in the past.

Specific Objectives:

- Measure and analyze the Raman spectra of the different external areas of the four vessels allows us to understand in a focused way the compounds with which they were manufactured, the manufacturing and environmental adversities, the physical-chemical information they contain, the places of origin and the use they had.

- Understand the importance of deconvolution to eliminate or reduce the noise of the analysis of each of the peaks obtained for its corresponding compound. Also, understand that for each spectrum it is necessary to use a function that correctly adjusts the obtained spectrum. Understand the delicate procedure of performing deconvolutions in order to obtain the best results.

- Compare the different spectral peaks in order to make a correct assignment based on the different data obtained. Assigning peaks of our spectrum and comparing them to each other gives us tools to check the use of elements and compounds for the manufacture of the archaeological pieces founded in the Caranqui area

- Detect vibrational and rotational states of the molecular system of our samples to probe their chemical composition and de functional groups. Compare the information obtained to analyze which functional groups the composition of our samples belongs to.
- Use the information obtained to verify the origin of the different vessels obtained. Study the composition of these vessels to promote the use of these archaeometric techniques in archaeological studies in our country. Consolidate and promote the importance that these studies provide to the community.

Chapter 5
Methodology

5.1 Raman Spectrometer

Instrumentation and Experimental Techniques

This section shows the structure of a Raman spectroscopic system. The instrumentation of these systems has optical and electrical components. The most important parts of a Raman spectroscope are described below.

5.1.2 Major Components

Four major components make up the commercially available Raman spectrometer[13]. These consist of the following:

A. Excitation source, which is generally a continuous-wave (CW) laser.
B. Sample illumination and collection system.
C. Wavelength selector.
D. Detection and computer control/processing systems.

A. Excitation sources

Elaborate systems were developed to supply a single wavelength with enough power to produce Raman scattering[13]. Lasers are ideal excitation sources for Raman spectroscopy due to the following characteristics of the laser beam:

1. Single lines from large CW lasers can easily provide 1-2 W of power, and pulsed lasers produce huge peak powers on the order of 10-100 MW.
2. Laser beams are highly monochromatic.
3. Most laser beams have small diameters (1-2 mm), which can be reduced to 0.1mm by using simple lens systems.
4. Laser beams are almost completely linearly polarized and are ideal for measurements of depolarization ratios.
5. It is possible to produce laser beams in a wide wavelength range by using dye lasers and other devices.

B. Sample Illumination

Since the Raman scattering is inherently weak, the laser beam must be focused properly onto the sample and the scattered radiation collected efficiently. The focusing of the laser onto the sample can be readily achieved because of the small diameter of the laser beam (~ 1 mm). Excitation and collection from the sample can be accomplished by using several optical configurations[13].

C. Wavelength Selectors

Wavelength selectors can be classified into several categories. The simplest device is an interference filter, which depends on its two optically flat surfaces to generate a constructive interference and transmit an integer number of wavelengths corresponding to twice the thickness of the filter[13]. Interference filters are constructed for single wavelengths (wavelengths corresponding to this wavelength divided by integers also will have constructive interferences and be observed). Variable, wedge-shaped interference filters are available for selecting desired wavelengths; however, the spectral resolution of these devices is generally too large for Raman spectra. Recently, acoustic and liquid-crystal tunable filters have been used successfully for measuring Raman spectra and Raman spectral images[1, 13].

D. Detection

Since Raman signals are inherently weak, the problems involved with detection and amplification are severe. Most of the very early work was performed with photographic detection using long exposure times. Furthermore, the time to develop photographic plates and examine them with a microphotometer rendered Raman spectroscopy unfit as a routine technique. This situation has changed considerably since the development of strong laser sources and sensitive detection techniques[13].

5.2 Raman Spectrometer used for the Analysis

The Raman equipment used for the measurement were*:* Raman *XploRA*.

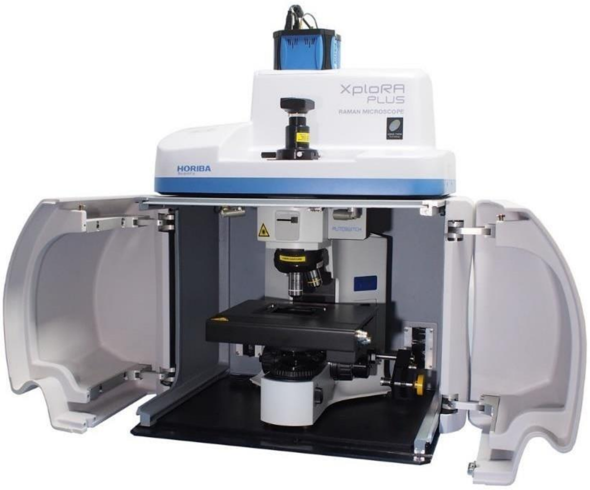

Figure 5.1: Raman XploRA Spectrometer equipment used for the measurements. Image adapted from Sestak et al. [26]

Measurements were performed at the University of Berlin in laboratories equipped with the Raman *XploRA* spectrometer. This spectrometer has several features: confocal imaging (0.5 μm XY), standard and high resolution and multilaser options (532, 638, 785 nm).

The following arrangement is a typical configuration of the components represents for a confocal Raman Spectrometer. The major categories for different instruments are defined by the wavelength region for the excitation sources, the type of wavelength selector, and the detection system. Most of the instrumentation will have similar sample illumination and collection systems.

Figure 5.2 shows a schematic diagram of a confocal Raman spectrometer. Adapted to Horiba *Raman XploRA* spectrometer model.

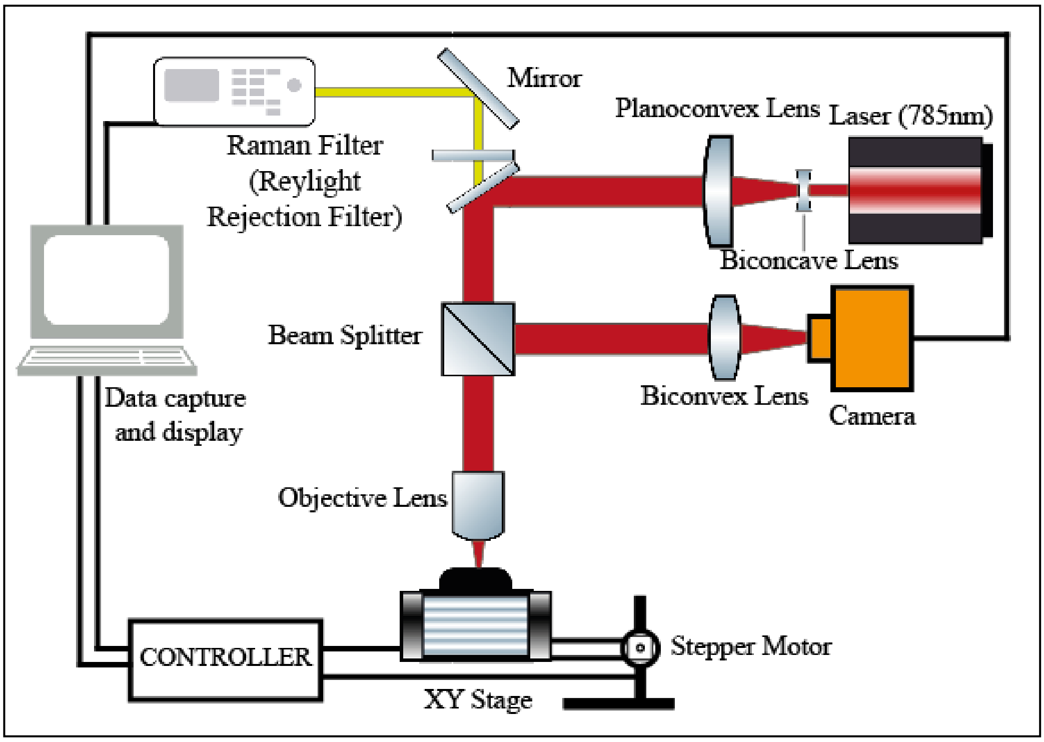

Figure 5.2: Diagram Scheme of configuration of the Confocal Raman spectrometer. Image adapted from Zhou et al. [27]

Raman Spectrometer Characteristics

Vessel measurements were performed with a 785nm laser. Due to the difficulty of analysis by the samples, we need to perform a high-resolution analysis. The spectral resolution is one of the most important factors to think about when acquiring a Raman spectrum. Defined as the wavenumber, wavelength, or frequency difference of two still distinguishable lines in a spectrum, spectral resolution requirements vary depending on the information one would like to obtain. The high spectral resolution is not always necessary for routine identification and analysis. However, if information about material properties, such as polymorphism, stress/strain, crystallinity, hydrogen bonding, and/or protein folding is to be obtained, high spectral resolution is necessary. The reason for this is that changes in these material properties can vary subtly alter the shape and/or position of the Raman peaks, which may not be detectable with lower spectral resolution.

Typical gratings used in Raman spectrometers vary from about 300 gr/mm (low resolution) up to 1800 gr/mm (high resolution) [26]. The HORIBA *XploRA* PLUS includes four automatically switchable and movable gratings (600 gr/mm, 1200 gr/mm, 1800 gr/mm, and 2400 gr/mm) [26]. For our measurements we used a 1200 gr/mm grating. We can see these parameters in more detail in Table 5.1.

Sample	***Equipment***	***Grid (gr/mm)***	***Scan Time (s)***	***Acquisition time (s)***	***Objective Lens***
1-1CLAY	*R.S XploRA*	*1200*	*5*	*20*	*50x*
2-1CLAY	*R.S XploRA*	*1200*	*10*	*30*	*50x*
3-1CLAY	*R.S XploRA*	*1200*	*10*	*30*	*50x*
4-1CLAY	*R.S XploRA*	*1200*	*10*	*30*	*50x*

Table 5.1: Raman measurements parameters in the region 785nm of different samples vessels.

The power used to make these measurements was 0.1%. For the 1-1CLAY sample, we performed 5 seconds of acquisition and 20 repetition cycles. For the 2-1CLAY, 3-1CLAY and 4-1CLAY samples we performed 10 seconds of acquisition and 30 repetition cycles.

5.3 Fitting Methods and Spectrum Analysis

5.3.1 Fitting Method

PeakFit v4.12

PeakFit is a Software that allow us compute the least-squares minimization curve fit for arbitrary, user-defined composite peak models. It outputs the best fit parameters for the defined model and the resulting total fit.

For this work, version v4.12 of PeakFit was used and was developed with the use of different functions that PeakFit offers us. To obtain the figures of the Section 6.4. from Chapter 6. we use the Voigt function (Amplitude, Gaussian/Lorentzian Widths):

$$y = \frac{a_0 \int_{-\infty}^{\infty} \frac{exp\,(-t^2)}{\frac{a_3^2}{2a_2^2} + \left(\frac{x - a_1}{\sqrt{2}a_2} - t\right)^2} dt}{\int_{-\infty}^{\infty} \frac{exp\,(-t^2)}{\frac{a_3^2}{2a_2^2} + t^2} dt}$$

where $a0$ = amplitude; $a1$ = center; $a2$ = width 1, Gaussian (> 0); a3 = width 2, Lorentzian (≥ 0).

PeakFit offers amplitude and area forms for a Voigt parametrization that directly computes the Gaussian and Lorentzian widths. This enables you to get a standard error and confidence limits for the computation of each of the widths[28].

With PeakFit tools, the option to vary widths affects the $a2$ parameter and the option to vary shape affects the $a3$ and higher parameters in the Voigt function. The changes in the width and shape can be treated picking the options of sharing and blocking. With these tools we can construct better peak for our analysis[28].

To have a reference of how the Voigtian function works, we make a brief introduction of its most important parts as well as its most characteristic properties.

Computation of Voigt Function

The Voigt functions are shown containing integrals simply because the convolution integrals lack real closed form solutions. There are, however, closed form complex solutions. PeakFit implements these complex analytical closed-form solutions, and as a result, computes exact Voigt functions to $|\varepsilon| < 1E - 14$ (to at least 14 significant figures). The Voigt function is now computed as accurately as a Gaussian, to full precision[28].

Spectral Fitting Considerations

When fitting spectral peaks, the x variable must be proportional to frequency, wave number, or energy. The variable must be a quantitative measure. As such, you must convent wavelength to wave number and transmission to absorption prior to fitting[28].

Deconvolution

Although “deconvolution” seems to be inappropriately applied to all peak fitting, with the Voigt a true deconvolution does occur, and in a manner that no noise is introduced into the analysis. The fitted parameters in G/L forms directly produce the deconvolved Lorentzian and instrument response function width. Because convolution of an instrument response function is area invariant, one assumes that Lorentz (a_0, a_1, a_3) represents the true peak (as measured by a perfect instrument) [28].

Chapter 6
Results & Discussion

In this chapter, Raman Spectroscopy results are presented. It contains the details of the data treatment such as the software and function used to fit the data. Besides, comparative tables of spectra information, spectral graphics, vessels figure and fundamental information about the composition of our compounds.

6.1 Importance of this research and its contrast with the tolas of Caranqui

The urban parish of Caranqui is located three kilometers south of the city of Ibarra and five kilometers southwest of the Yaguarcocha lake. Actually, Caranqui with 15,500 habitants, has been recognized for centuries as the ancient center of the canton Ibarra and its surroundings. Recent archaeological data from the central area of the town provide evidence of an occupation that stretches from at least 2000 years into the past[29].

To have a historical idea of Caranqui, we have to go back to the past to build a timeline that allows us to analyze the historical ethnic processes that this town had. For this reason, I develop this research starting from the time when the highlands of Pichincha, Imbabura and Carchi were an important part of the Inca empire, before the Spanish invasion.

Early documentary sources generally agree that it was Topa Inga Yupanqui who made the initial forays into this region but that it fell to his son, Huayna Capac, to firmly establish control here[30]. The northern frontier was, in fact, the main focus of military efforts during the final decades of the Inca Empire's existence, consuming the bulk of Huayna Capac's attention and resources. Somewhat surprisingly though, discussion of this region is often omitted or only minimally included in the larger narratives of Tawantinsuyu. Recent investigations at the late imperial site of Inca-Caranqui, located at the northernmost edge of Tawantinsuyu, are aimed precisely at elucidating the history and significance of this frontier region within the overall agenda of the Inca Empire during the later phases of conquest and expansion (Figure 6.1) [30].

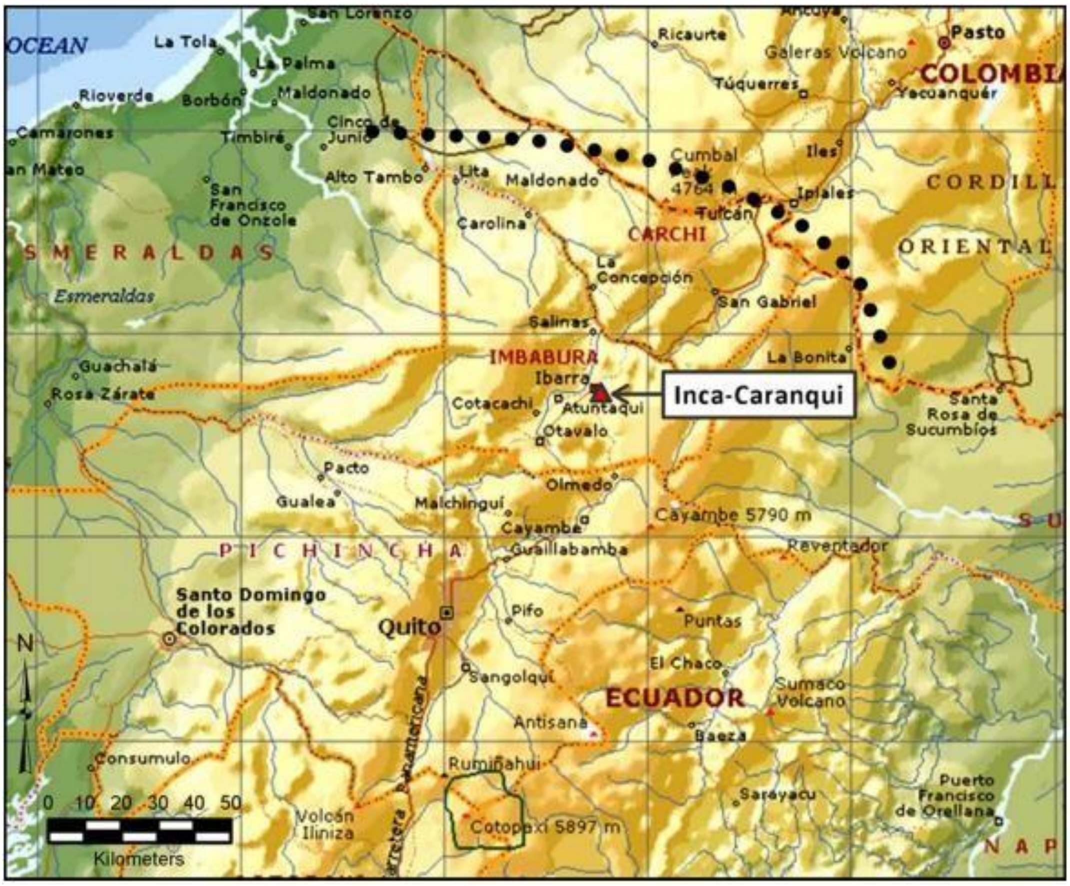

Figure 6.1: Map of northern Ecuador indicating northern limits of Tawantinsuyu (dotted line) and location of the site of Inca-Caranqui in Imbabura Province, Ecuador. Image adapted from Bray et al. [29]

The sum of the evidence suggests that imperial control over this region was patchy and tenuous till the end, that the military strategy of the invaders was to isolate the recalcitrant Caranqui-Cayambe population, and that this strategy resulted in the Inca's ability to execute a final, multipronged attack that left them at last victorious. The Caranqui Wars likely ended sometime between 1518 and 1522[30].

The territory comprising the northern frontier of Tawantinsuyu coincides with the northernmost provinces of modern Ecuador up to and including the Colombian border region (see Figure 6.1). During the late pre-Columbian era, and possibly much further back in time, the indigenous residents of this region appear to have spoken a common language, shared similar artistic traditions, practiced similar subsistence technologies, and followed comparable settlement strategies[29]. This can be seen in the regional toponymy, the use of similar raw materials, the types and styles of pottery produced, metalwork and lithic technologies, spatial patterning at both the domestic and community levels, and burial practices[30].

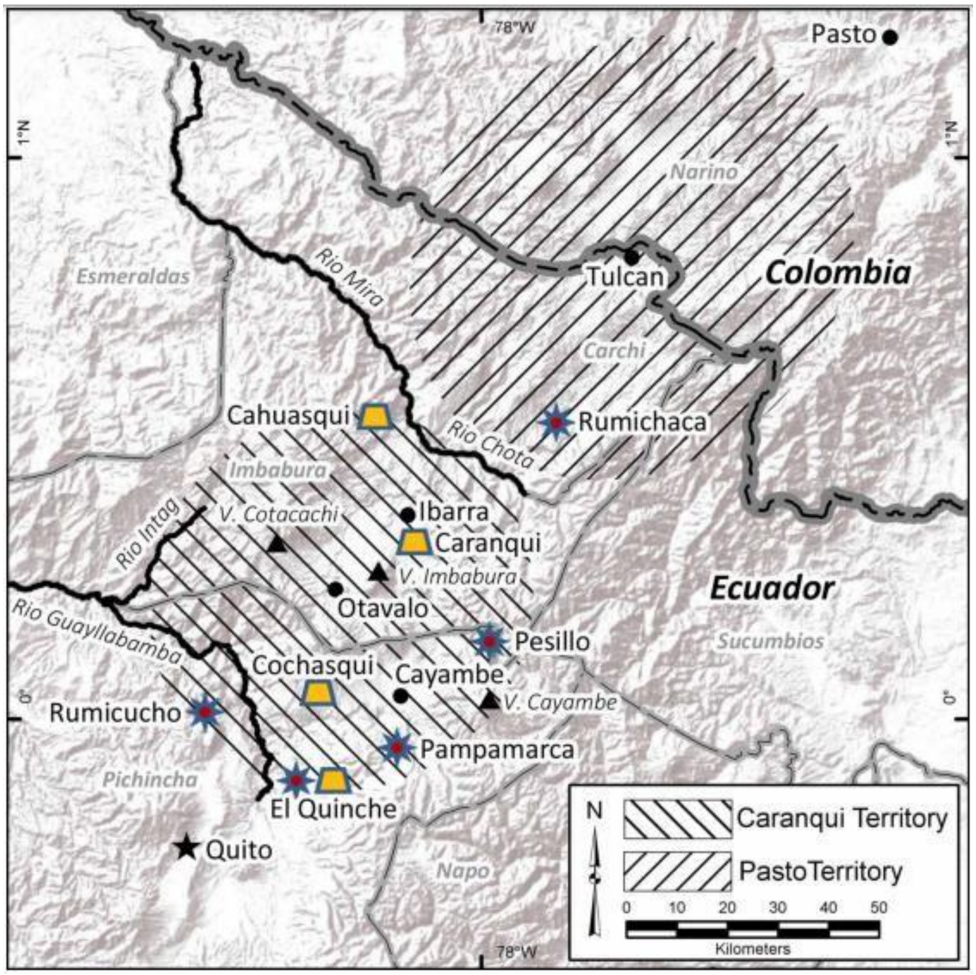

Figure 6.2: Map of northern Ecuadorian highlands indicating approximate extent of Caranqui and Pasto ethnic territories as well as sites, landmarks and modern towns. Blue stars indicate hilltop fortress (pucara) sites, and yellow trapezoids indicate mound (tola) sites. Image adapted from Bray et al. [29]

Caranqui once had at least 11 tolas and was the settlement most important part of the Inca empire at the northern end of the Tawantinsuyu probably due to its strategic location[29]. In Figure 6.2 the yellow trapezoids indicate the principal tolas sites.

The tolas were mounds that were of great importance in the Caranqui country and other settlements. These constructions have often been considered as favorite areas for religious or ceremonial functions, platforms for chief residences, commercial areas, ancestral cemeteries and probably served as periodic concentration centers for members of the dispersed community for social purposes[29].

Develop spectroscopy studies of the vessels from these areas allows us to know certain characteristics about the communities that used them. For example, it allows us to know the processes through which these materials passed, supply areas, if they had religious offering functions, food storage containers, tombstones or were used in the kitchen. The importance and mention of the tolas in this project is due to the fact that there were a greater number of settlements in the tolas and their surroundings. In addition, because the tolas were cacical areas, the offerings and commercial exchanges were made in containers made of clay. A large number of pots, vessels, amphorae and other objects made of clay have been found in the tolas located in Caranqui. The tolas are reference zones of great importance in the study of these ancient communities[29].

6.2 Vessels Location

The location of vessels A and B is shown in the Figure 6.3. The exact location of the vessels has the following coordinates: 820068.00 mE, 34421.00 mN. In Figure 6.3 we can observe the 17 tolas of the sector of the current parish of Caranqui.

These tolas are distributed in different areas and have a distribution according to a social classification. As we can see, EMAPA’s tola is located in the center, according to the characteristics in height, width and number of objects found in this tola, we discerned that Caranqui was a mid-range site within the curacazgo. Remember that that the largest and most crowded tolas belonged to caciques of high rank in terms of social classification. It is important to mention that the concentrations of the tolas are due to the caciques trying to choose the best places to settle. Due to this, there were "neighborhoods" of tolas where commercial areas, merchants and other services could be found.

In Figure 6.4 we observe the distances between the location where the vessels were found and the tolas closest to them. In this case the closest tolas were: Tola Valencia at 1.14km; Tola M. Torres at 1.1km; Tola A. Jiménez at 0.91km.

In the other hand, vessels C and D do not have an exact location, but were found in the Caranqui parish sector. In section 6.3 of this chapter I will present the necessary information to understand the importance of developing these studies for archaeological objects without initial referential information.

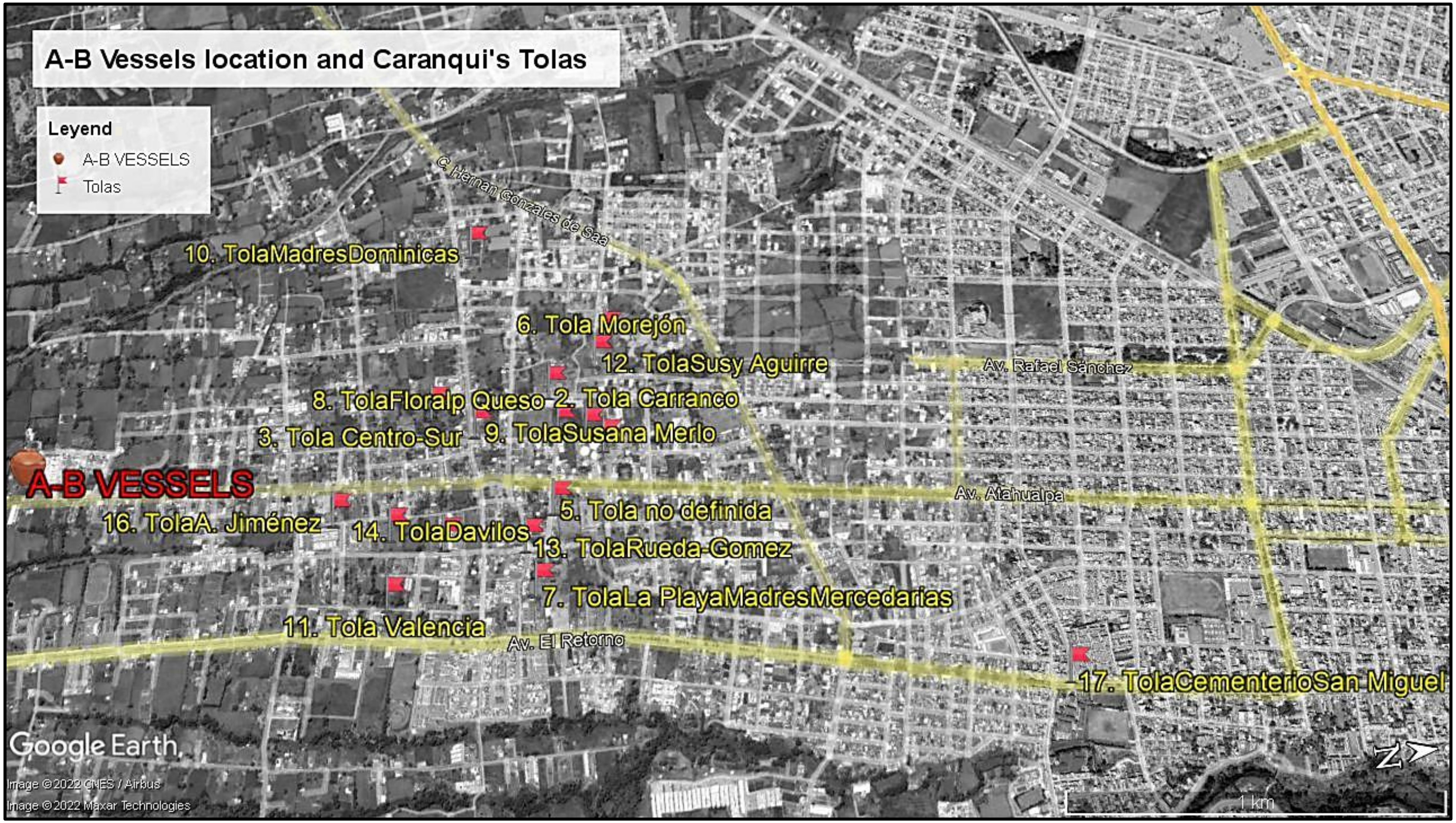

Figure 6.3: Map of vessels A and B with their geographic coordinates. The red flags represent the exact locations of each of the 17 tolas in Caranqui.

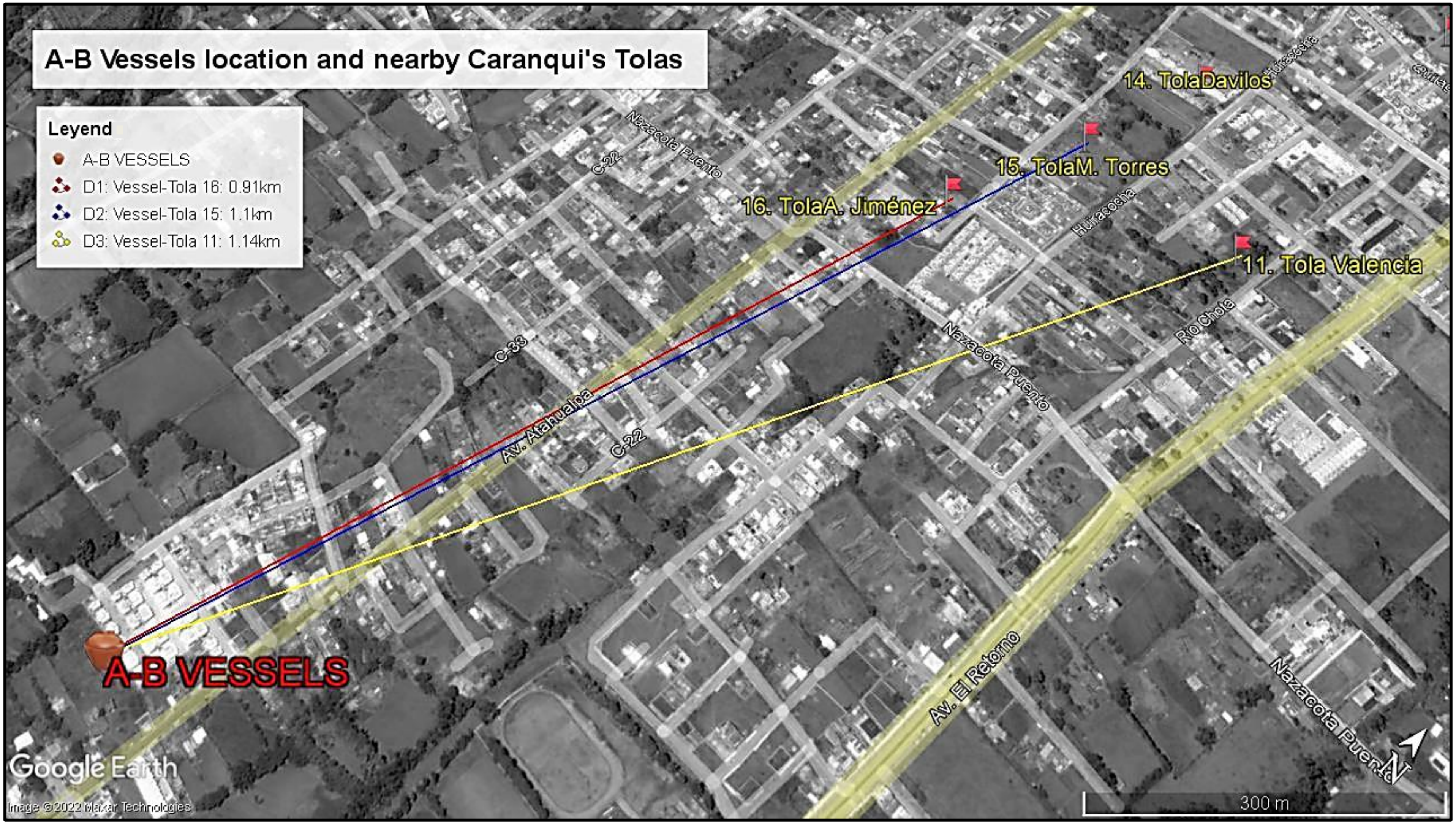

Figure 6.4: Map with the exact distances between the place where vessels A and B were found, and the closest tolas. Tola Valencia (11) at 1.14km; Tola M. Torres (15) at 1.1km; Tola A. Jiménez (16) at 0.91km.

6.3 Vessels Characteristics

The four vessels analyzed by the Raman spectroscopy technique can be seen in Figure 6.5. The characteristics of the vessels are detailed in Table 6.1.

Vessel	*Sample name*	*Type*	*Thickness (cm)*	*Width (cm)*	*Heigth (cm)*	*Sampling section*
A	*1-1CLAY*	*Pot*	*0,41*	*14,3*	*20*	*Lower external*
B	*2-1CLAY*	*Pot*	*0,5*	*10,5*	*30*	*Middle external*
C	*3-1CLAY*	*Jug*	*0,35*	*11,25*	*30*	*Lower external*
D	*4-1CLAY*	*Bowl*	*0,6*	*12,9*	*30*	*Lower external*

Table 6.1: Characteristics of the four vessels analyzed by the Raman spectroscopy technique: (A) Reddish-brown pot-type vessel with a narrow mouth and a thickness of 0.41 centimeters. The sampling section was taken, as we can observe in the yellow square, in the lower external area that shows signs of having been exposed to fire. (B) Black-gray pot-type vessel with a narrow mouth and a thickness of 0.5 centimeters. The sampling section was taken in the external middle zone that presents a dark color. (C) Reddish-orange jug-type vessel with a narrow mouth and a thickness of 0.35 centimeters. The sampling section was taken in the lower external area that shows signs of having been exposed to fire. (D) Reddish bowl-type vessel with an open mouth and a thickness of 0.6 centimeters. The sampling section was taken in the lower external area that has a dark color.

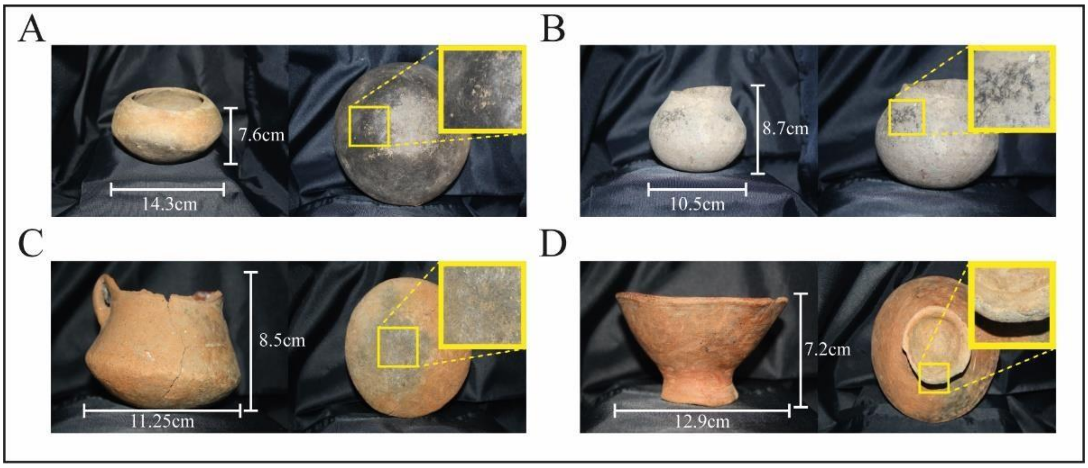

Figure 6.5: Photographs of the vessels and their respective sampling sections.

6.4 Vessels Raman Analysis

The Raman measurements were performed as it was mentioned in the Chapter 5 section 5.1.1, the data spectrums were analyzed with Peak-fit software and graphed by Origin software. The fitting of the specters of the vessels A (1-1CLAY), B (2-1CLAY), C (3-1CLAY), D (4-1CLAY) were made with the Voigt function (Amplitude, Gaussian/Lorentzian Widths). The Raman measurements of the vessels presented fluorescence which hide all the signals. This issue also has been reported by Michaelian[32] that solved it with a baseline correction and reducing the range of measurement. It also was reported that in powdered samples of clay minerals like Kaolinite it I more difficult to obtain good Raman signals[31]. Consequently, a base line correction with the software measurement was applied in all the Raman experiments for the clay samplings. In Table 6.2 observe the different baseline functions used to obtain better Raman signals.

	Vessel	*Sample name*	*Fitting Function*	*Baseline Correction Function*
1	**A**	*1-1CLAY*	Voigt (Amp, G/L)	*Quadratic Bg*
2	**B**	*2-1CLAY*	Voigt (Amp, G/L)	*Quadratic Bg*
3	**C**	*3-1CLAY*	Voigt (Amp, G/L)	*Logarithmic Bg*
4	**D**	*4-1CLAY*	Voigt (Amp, G/L)	*Logarithmic Bg*

Table 6.2: Fitting and Baseline Correction functions corresponding to each vessel sample.

The Raman measurements parameters in the region $785nm$ of the samples was presented in the chapter 5, section 5.1. In Table 5.1 observe the different values of grid, scan time, acquisition, objective lens and the hole aperture. As I mentioned in the chapter 5, we used a 1200 gr/mm grating, a power of 0.1%, for the 1-1CLAY sample, was performed 5 seconds of acquisition and 20 repetition cycles, and for the 2-1CLAY, 3- 1CLAY and 4-1CLAY samples it was performed 10 seconds of acquisition and 30 repetition cycles.

The sampling section for the measurements were different for each vessel (see Table 6.1 and Figure 6.5). A very important factor that should be mentioned is the specification of the sampling sections that were used for the analysis. Figure 6.5 shows the different sampling sections, but the specific area that was used for the analysis must be detailed. For vessel A, a sample was taken from the dark zone, presumably produced by exposure to high temperatures. The sample from Vessel B was taken from the dark area of this section. For vessel C, a sample was taken from the dark area of the section. Finally, for vessel D, a sample was taken from the gray area of its lower part.

The sampling sections taken to carry out the Raman spectroscopy analyzes were dark, it can be assumed that they were areas exposed to high temperatures, that is, they were close to fire. We will discuss this later.

The information obtained by the Raman spectroscopy technique for the four vessels can be seen in Figure 6.6. The region was analyzed in the range from 50 to $4000nm$. The four spectra obtained for samples 1-1CLAY, 2-1CLAY, 3-1CLAY and 4-1CLAY are observed. In the region from 50 to $500nm$, three prominent peaks are observed and others that are present in all the fittings of the spectra. The most important part of these spectra is the low frequency region because it contains a large amount of information (peaks). This spectral region will be discussed later in more detail.

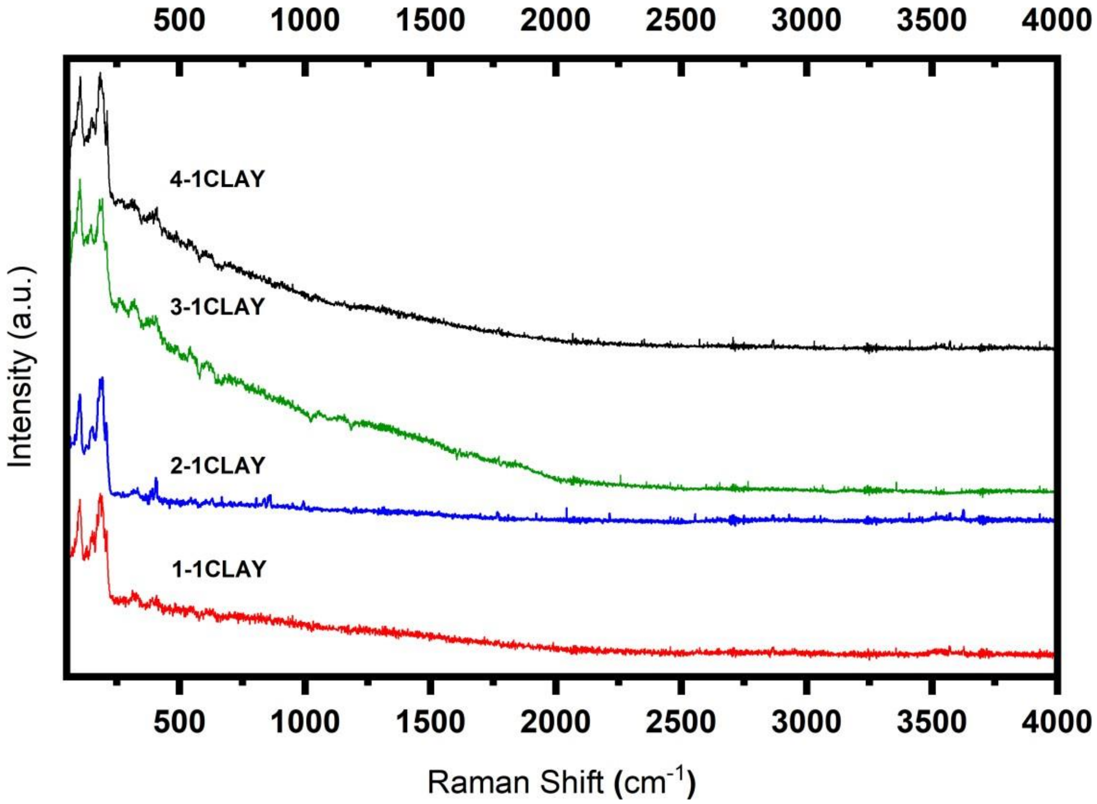

Figure 6.6: Raman spectrum region of samples subtracted from Caranqui-Inca period vessels found in Imbabura-Ecuador. Experimental conditions: excitation source, $785nm$. The most important region is the low frequency region because we have more information collected. Clay samples: 1-1CLAY, 2- 1CLAY, 3-1CLAY and 4-1CLAY. Raman Shift range between $50cm^{-1}$ to 4000 cm^{-1}.

In Figure 6.7 the region spectra analyzed is between 70 to $1000nm$. In these spectra the background was subtracted with different functions. As mentioned by Michaelian[32], background subtraction by software is a good mechanism to obtain good Raman analyses. In this way we use different functions in order to obtain a better data analysis (see Table 6.2). Each spectrum has different structures that can give us graphs with large dispersions. It is essential that a suitable function is used to subtract the background.

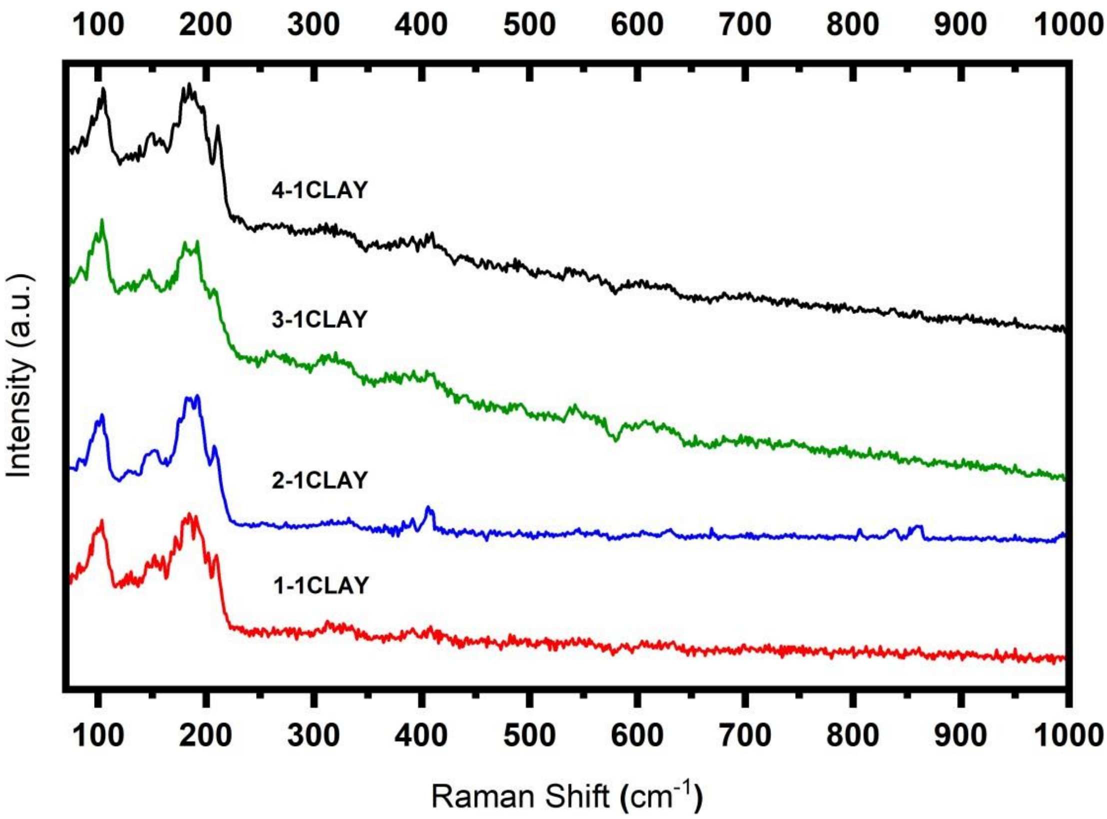

Figure 6.7: Raman spectrum region of samples subtracted from Caranqui-Inca period vessels found in Imbabura-Ecuador. Experimental conditions: excitation source, $785nm$. Clay samples: 1-1CLAY, 2-1CLAY, 3-1CLAY and 4-1CLAY. Raman Shift range between 70 cm^{-1} to $1000cm^{-1}$. The background was subtracted by PeakFit software functions. For 1-1CLAY and 2-1CLAY the Quadratic function subtracted the background. For 3- 1CLAY and 4-1CLAY the Logarithmic function subtracted the background.

6.4.1 Deconvolution

This section presents the deconvolutions of the spectra of the samples: A: 1-1CLAY, B: 2-1CLAY, C: 3-1CLAY and D: 4-1CLAY. The spectral region analyzed is between $66cm^{-1}$ to $500cm^{-1}$. In each of the graphs it is observed that each peak of the deconvolution belongs to a specific element. As mentioned above, the study of this spectral region was developed with a high spectral resolution in order to have the necessary information to analyze the elements present in each of the samples.

It is very important to understand that performing the deconvolution of our spectrum analyzes allows us to have a better appreciation of the information collected. Deconvolution techniques currently available for application in spectroscopy must presuppose a known system response function. An inexactly presupposed response function can degrade the obtainable resolution of instruments[33].

The spectra plotted by Origin give us relevant information about the most prominent peaks of each compound. In Figure 6.8 we can see the graphs of the spectra obtained for all the samples. Each of the deconvolutions contains peaks that represent a specific compound in the spectral region analyzed.

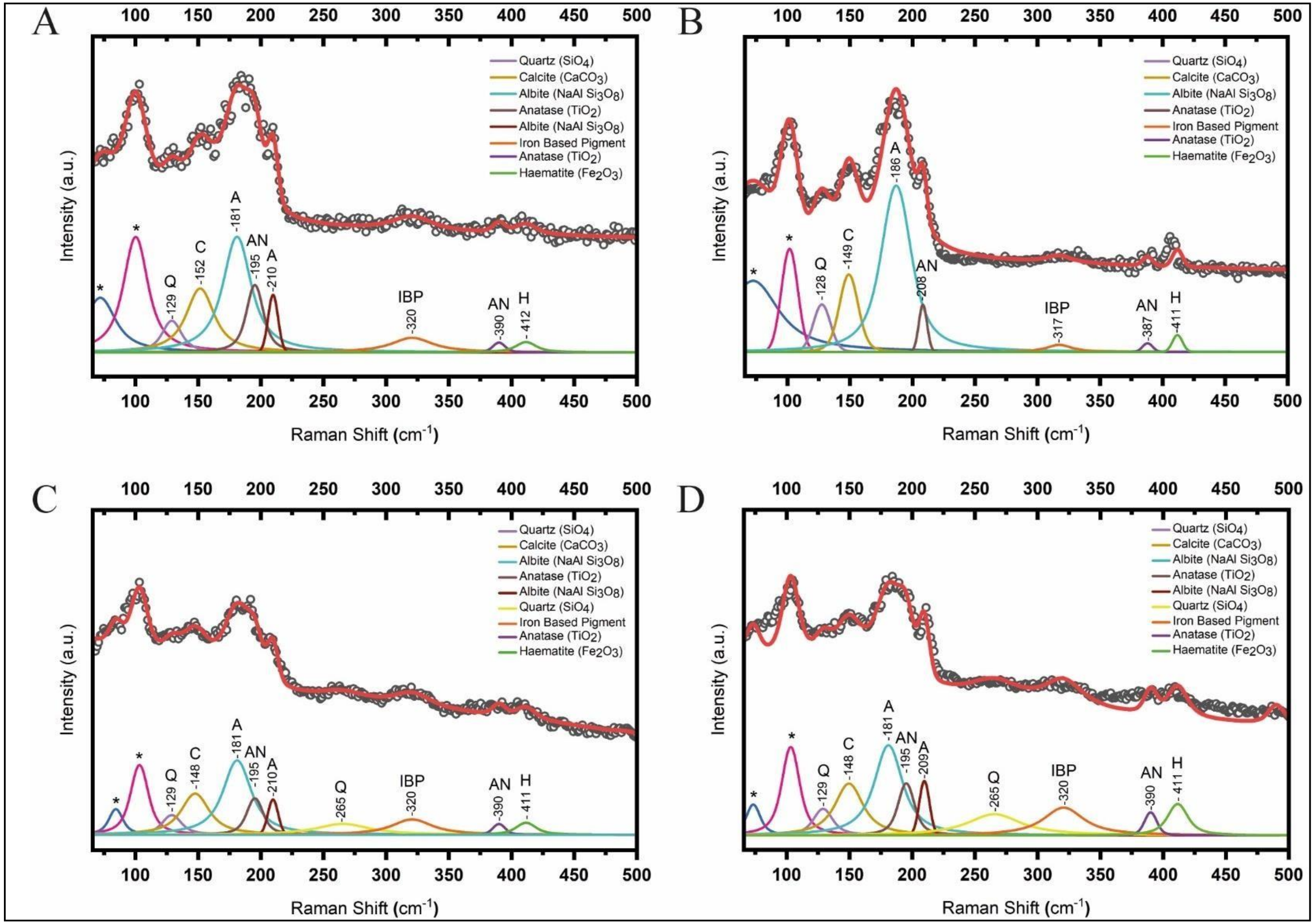

Figure 6.8: Raman spectrum region and their respective deconvolutions of samples subtracted from Caranqui-Inca period vessels found in Imbabura-Ecuador. Experimental conditions: excitation source, 785nm. Clay samples: A: 1-1CLAY; B: 2-1CLAY; C: 3-1CLAY; D: 4-1CLAY. Raman Shift range between 66cm^{-1} to 500cm^{-1}. Each peak corresponds to a different compound: Q: Quartz; C: Calcite; A: Albite; AN: Anatase; IBP: Iron Based Pigment; H: Haematite.

Compound or element name	***Description***	***Reference Wavenumber value (cm^{-1})***	***Sample Measurement Value (cm^{-1})***
α-Quartz	*- Silicate (SiO_4)* *Three-dimensional polymer* *Tetrahedral.*	*126*	*A: 1-1CLAY (129)* *B: 2-1CLAY (128)* *C: 3-1CLAY (129)* *D: 4-1CLAY (129)*
		262	*C: 3-1CLAY (265)* *D: 4-1CLAY (265)*
Calcite	*Calcium carbonate ($CaCO_3$)* *Carbonates and nitrates.* *Rhombohedral.*	*155*	*A: 1-1CLAY (152)* *B: 2-1CLAY (149)* *C: 3-1CLAY (148)* *D: 4-1CLAY (148)*
Albite	*- Tectosilicates ($NaAlSi_3O_8$)* *Silicates, subgroup tectosilicates and feldspars* *Triclinic, pinacoidal.*	*183*	*A: 1-1CLAY (181)* *B: 2-1CLAY (186)* *C: 3-1CLAY (181)* *D: 4-1CLAY (181)*
		210	*A: 1-1CLAY (210)* *B: 2-1CLAY (208)* *C: 3-1CLAY (210)* *D: 4-1CLAY (209)*
Anatase	*Titanium dioxide (TiO_2)* *Oxides* *Tetragonal, dipyramidal ditetragonal class*	*196*	*A: 1-1CLAY (195)* *C: 3-1CLAY (195)* *D: 4-1CLAY (195)*
		396	*A: 1-1CLAY (390)* *B: 2-1CLAY (387)* *C: 3-1CLAY (390)* *D: 4-1CLAY (390)*
Iron-Based Pigment	*Iron Oxides* *(FeO, Fe_2O_3, Fe_3O_4)* *Oxidation or reduction cycles of iron oxides* *- Maghemite ($\gamma - Fe_2O_3$)* *Magnetite, Hematite* *Black/brownish decors*	*317*	*A: 1-1CLAY (320)* *B: 2-1CLAY (317)* *C: 3-1CLAY (320)* *D: 4-1CLAY (320)*
	- Hematite ($Fe_2O_3, \alpha - Fe_2O_3$) *Iron Oxides* *Scalenohedral hex*	*410*	*A: 1-1CLAY (412)* *B: 2-1CLAY (411)* *C: 3-1CLAY (411)* *D: 4-1CLAY (411)*

Table 6.3: Descriptions, measured values of the samples and reference values of each element or compound.

Peaks from the same compounds have the same color on each plot.

Firstly, for graph A, we have ten different peaks. Two of the peaks were not assigned because no referential information was found about ceramics excited in that spectral region with a $785nm$ excitation source. Moreover, we have low intensity Quartz (Q) at $129cm^{-1}$, Iron oxides (IBP) at $320cm^{-1}$, Anatase (AN) at $390cm^{-1}$ and Haematite (H) at $412cm^{-1}$. Also, at high intensities we have Calcite (C) at $152cm^{-1}$, Albite (A) at $181cm^{-1}$ and $210cm^{-1}$, and Anatase (AN) at $195cm^{-1}$. For graph B, we have nine different peaks. Two of the peaks were not assigned because no referential information was found about ceramics excited in that spectral region with a $785nm$ excitation source. Moreover, we have low intensity Quartz (Q) at $128cm^{-1}$, Iron oxides (IBP) at $317cm^{-1}$, Haematite (H) at $411cm^{-1}$ and Anatase (AN) at $387cm^{-1}$. Also, at high intensities we have Calcite (C) at $149cm^{-1}$, Albite (A) at $186cm^{-1}$ and $208cm^{-1}$. For graph C, we have eleven different peaks. Two of the peaks were not assigned because no referential information was found about ceramics excited in that spectral region with a $785nm$ excitation source. Moreover, we have low intensity Quartz (Q) at $128cm^{-1}$ and $265cm^{-1}$, Iron oxides (IBP) at $320cm^{-1}$, Anatase (AN) at $390cm^{-1}$ and Haematite (H) at $411cm^{-1}$. Also, at high intensities we have Calcite (C) at $148cm^{-1}$, Albite (A) at $181cm^{-1}$ and $210cm^{-1}$, and Anatase (AN) at $195cm^{-1}$. For graph D, we have eleven different peaks. Two of the peaks were not assigned because no referential information was found about ceramics excited in that spectral region with a $785nm$ excitation source. Moreover, we have low intensity Quartz (Q) at $129cm^{-1}$ and $265cm^{-1}$, Iron oxides (IBP) at $320cm^{-1}$, Anatase (AN) at $390cm^{-1}$ and Haematite (H) at $390cm^{-1}$. $411cm^{-1}$. Also, at high intensities we have Calcite (C) at $148cm^{-1}$, Albite (A) at $181cm^{-1}$ and 209 cm^{-1}, and Anatase (AN) at $195cm^{-1}$. All this information is contained in the Table 6.3.

The detection of different clay minerals is almost prevented if iron oxides (such as hematite) and/or titanium oxides (such as anatase) are admixed to the sample, because of the high sensitivity of Raman spectroscopy to these types of minerals. Both of them represent common admixtures in natural earths[34].

Albite

The results show us that the four vessels are made of materials that contain the same compounds except for sample 2-1CLAY in which Anatase (AN) is not present in 195cm- 1, and Quartz (Q) in 265cm-1 of the spectrum corresponding to the sample 3-1CLAY and 4-1CLAY. Figure 6.8 shows that the peaks with the highest intensities correspond to Albite (A). This compound constitutes the sodium endmember of both the plagioclase and the alkali feldspar series[35]. The observation of albite in our samples allows us to draw conclusions on the firing temperature. The six bands at 183 (w), 210 (w), 292 (m), 457 (w), 480 (m) and $508cm^{-1}$(s), marked with A on the spectrum, are in good agreement with the band wavenumbers reported for low temperature albite[37]. Albite belongs to Tectosilicates ($NaAlSi_3O_8$) minerals and its crystal system is triclinic, pinacoidal[38]. Albite is a feldspar characterized with the lowest concentration of Ca[23]. Observe the Table 6.3 to compare the wavenumbers excitation obtained in this analysis and the reference values. Phases with high Ca concentrations are formed above 950 °C[39], as a result of decomposition of Calcite ($CaCO_3$). Spectra of Calcite ($CaCO_3$) were detected separately in the pottery shards examined (see Figure 6.8: A; B; C; D). The fact that we observed only low-temperature albite indicates that the firing temperature was below 950 °C[23]. Consequently, vessels A, B, C and D contain two excitation bands at 181cm^{-1} and 208cm^{-1}.

Calcite (C)

Calcite (C) or calcium carbonate ($CaCO_3$) belongs to carbonates and nitrates, and its crystal system is rhombohedral[38]. This mineral is part of the temper in the clay from which the pottery pieces were made, most probably ground-up shells[33]. The four bands at 155(w), 281(m), 712 and 1085cm^{-1} (s) are in agreement with the band wavenumbers of the Raman-active modes of calcite belonging to the trigonal space group D^6 [38]. In addition, calcite can be a result of a post-burial deposition process. The fact that in our samples it exists as part of the temper $_{3d}$ confirms the suggestion made earlier that this pottery was fired at relatively low temperatures, below the decomposition temperature of calcite, as mentioned, which is around 950 °C[33].

α-Quartz (Q)

Another mineral very present in this study is quartz (Q). α-Quartz, is commonly found in ancient ceramics[40]. It is a three-dimensional polymer in which the SiO_4 tetrahedral units are linked throughout the crystal. The spectrum is characterized by a symmetric bending vibration ($Si–O–Si$) at 463 cm^{-1} strong band, medium to weak bands due to lattice modes at 126, 199 and 262 cm^{-1} and weak bands at 356 and 401 cm^{-1} due to asymmetric bending modes of the silica tetrahedra[33]. For this study the medium weak bands analyzed were 126 and 262 cm^{-1}. The 126 cm^{-1} medium weak band is present in the four vessels samples and the 262 cm^{-1} is present only in 3-1CLAY and 4-1CLAY samples. It is the typical and majority mineral of some magmatic rocks, such as granite, diorites, andesites and others[33].

Anatase (AN)

Anatase, or titanium dioxide *(TiO_2),* belongs to an oxide mineral. Has a tetragonal, dipyramidal ditetragonal crystal system[36]. It is characterized by a strong band at 144 cm^{-1} and three weaker ones at 396, 515 and 639 cm^{-1} and one very weak band at 196 cm^{-1} (see Figure 2.30). This anatase analysis is based on the weaker band at 396 cm^{-1} and the very weak band at 196 cm^{-1}. High Raman scattering of anatase results from covalent character of $Ti - O$ bonds in anatase's lattice. The intensity of the main anatase band at 143–154 cm^{-1} is further increased by the high symmetry of the $O - Ti - O$ bending vibration[41]. Most probably anatase mineral was part of the clay composition used for the vessels. The presence of anatase in the samples suggests a firing temperature below the anatase–rutile transition point (750–950 °C), which depends on various factors including the iron concentration[36]. Anatase is present in all Raman spectra, except for sample 2-1CLAY, where only have a peak at 387 cm^{-1} that corresponds to the weaker band.

Iron-based Pigments (IBP)

The pigment colors of our samples from black, red and reddish are discussed in this section. Iron-based pigments, depends of the oxidation conditions. It is very important, because the oxidation state of iron is strongly dependent on the atmosphere under which ceramic was fired[42]. Due to all of our vessels have red, black/brownish, and burnt colours, information necessary to understand the pigmentation or cause of their colour is presented.

For black pigment a reducing atmosphere in the kiln is an important condition for the formation of these colour surface[43]. Thus, the presence of either natural organic or added carbonaceous material will fire black in colour under these conditions due to the formation of carbon. But it is also a requirement that kiln temperatures must be lower; otherwise, oxidation of carbon to carbon dioxide occurs[47]. On the other hand, ferruginous clays that contain iron oxides and hydroxides can form spinel phases that are mainly black in colour[44]. In the spectra reported in Figure 6.8 and obtained on the black/brownish vessels, one can observe a spectral band centered around 317 ±3 cm^{-1} for Iron Oxides, and 410 ±1 cm^{-1} for Hematite. This spectrum could represent a reaction intermediate formed during the oxidation or reduction cycles of iron oxides[45].

The reddish trivalent iron oxide (e.g. hematite) is formed under an oxidizing atmosphere[44]. According to the crystal space group to which hematite belongs (D_{3d}^{6}), two A_{1g} modes at 225 and 498 cm^{-1} and five E_g modes at 247, 293, 299, 412 and 613 cm^{-1}, respectively [43]. Red pigments, also can be seen where the spectral characteristics of the mineral hematite ($\alpha - Fe_2O_3$), were observed as follows: A total of six out of seven possible Raman-allowed modes: the phonons corresponding to A_{1g} modes (225 and 496 cm^{-1}) and E_g modes (244, 293,410 and 612 cm^{-1}) [45].

How the black and red coatings were produced remains a major question and has engendered much discussion over the years. The process, as rediscovered by Theodor Schumann[43] in 1942, was based on the influence of the kiln atmosphere on the kind of iron oxide produced. Attic clays are rich in iron oxides and they become red in colour when they are fired in an oxidizing atmosphere and black when the kiln atmosphere is a reducing one. This black and red pottery is produced in a three-step process. During the first oxidizing step of the firing, both the clay and the glaze material, obtained from the clay, turned red. In the next reducing step, both turned black. Finally, in the next reoxidizing step the porous red-fired clay again turned red but the glaze, due to the fact that it had sintered and sealed off the black iron oxide from contact with the oxygen in the air, did not reoxidize to a red colour. The presence of this residual magnetite on the final red surface, as indicated above, highlights the fact that the reoxidizing step is not a complete process. The amount of residual magnetite will depend on several factors: the types of clays employed, the temperature and atmospheric conditions in the kiln, and so on[43].

In yellow, brown and red earths, the colour is caused by the presence of free ferric oxides in the form of admixtures of white clay minerals. The final hue can be further influenced by other admixtures, such as e.g. manganese oxides[46]. The technical term "ochre" (originally related to the colour), which is widely used in archaeometry and conservation science as alternative to the term "earth", should be considered as more general covering all natural iron-based pigments, even those containing no clay minerals as being products of oxidation of sulphides and not silicates[46].

6.5 Comparative Analysis

Archaeometry is the study of archaeological objects through different techniques. For this work, the analysis of four different vessels found in Caranqui has been developed, after obtaining their respective studies we can understand that most of our compounds contain similar materials with some exceptions. According to the archeometrists, the works vary from hand-made to wheel-made. The clays may be described as originating from well-mixed, fine, sandy, sedimentary clays, fired, surface slipped then painted or polished[33].

Raman spectroscopy is a powerful analytical method for non-destructive material characterization. In the past 7 years, there has been a notable increase in the number of studies applying the Raman spectroscopic technique to archeological artifacts ranging from Egyptian funerary artifacts, mummies, to prehistoric rock, art, byzantine hagiography, medieval paintings, manuscripts, cantorals and various objects of fine art from more recent history[33]. In the cultural heritage research, their interpretative potential remains almost completely unexploited (particularly in the field of analysis of historical paintings) mainly due to the following reasons: (i) an almost absence of geological- mineralogical approach in the analysis of fine art and (ii) lack of suitable methodology of clay microanalysis[34].

Košařová, Hradil, Němec, Bezdička and Kanický[34] performed Raman spectroscopic analyzes of different samples as natural clay pigments including white clay minerals (kaolinite, illite, montmorillonite), green earths (glauconite and celadonite) and red earths (natural mixtures of white clay minerals with hematite). For the samples of red earths, hematite (Fe_2O_3) is usually present as a coloring admixture of white clay minerals. The Raman spectra of pure hematite measured with 532 and 785nm lasers (Figure 6.9) exhibited characteristic bands in the 200–700 cm^{-1} region. This hematite is a synthetic hematite (powder pigment) [34] .Raman bands occurring at 611, 497, 411, 293, 245 and 225 cm^{-1} are assigned to the $Fe - O$ stretching[34].

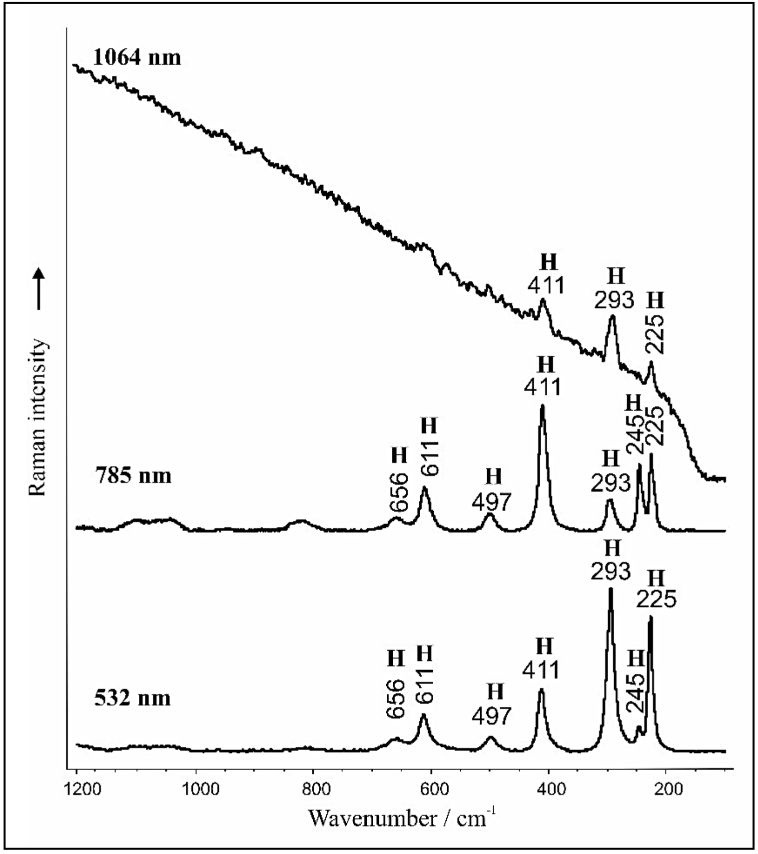

Figure 6.9: Raman spectra from sample M140, Fig. S1 supporting information. Red earth composed by synthetic hematite (powder pigment) (H = hematite). Image adapted from Košařová et al. [34]

As we mentioned in section 6.4.1, for hematite in our analysis we obtained excitations in the Raman bands of 412 cm^{-1}, corresponding to the 1-1CLAY sample; 411 cm^{-1}, corresponding to samples 2-1CLAY; 3-1CLAY; 4-1 CLAY. Something important that should be mentioned are the conditions to which the ceramic was exposed. It is essential to understand the processes through which it went through over time[42]. The temperature, atmospheric pressure, mixing conditions, and others, are essential to relate the objects analyzed in these works[43]. In addition to this, there are several relationships in obtaining the compounds but at different bands. The spectral features could become similar, but they went through different processes and conditions. To understand this, we need to understand that each compound reacts differently to intensity, power, acquisition time, scan time, the grid and other parameters.

For reds clays, the sample *K40500* in Figure 6.10 is one of the best to analyze α- quartz. This is a Red earth from Bavaria, Germany (powder pigment)[34]. A strong band at 462 cm^{-1} together with a weak band at 200 cm^{-1} using were found. Quartz belongs among three-dimensional polymers with SiO_4 tetrahedral units linked throughout the crystal[33]. As we discuss in the section 6.4.1, Raman spectrum of α-quartz in natural earths is characterized by a prominent band at 463 cm^{-1}, which is assigned to asymmetric bending of $O - Si - O$ bond inside the SiO_4 tetrahedron. Certainly, in our analysis we did not find a strong band reference. Conversely, we obtained bending vibration in the weak and medium bands at 128 ±1 for the four samples, and 265 cm^{-1} for 3-1CLAY and 4-1CLAY, in reference to 126 and 262 cm^{-1}, correspondly.

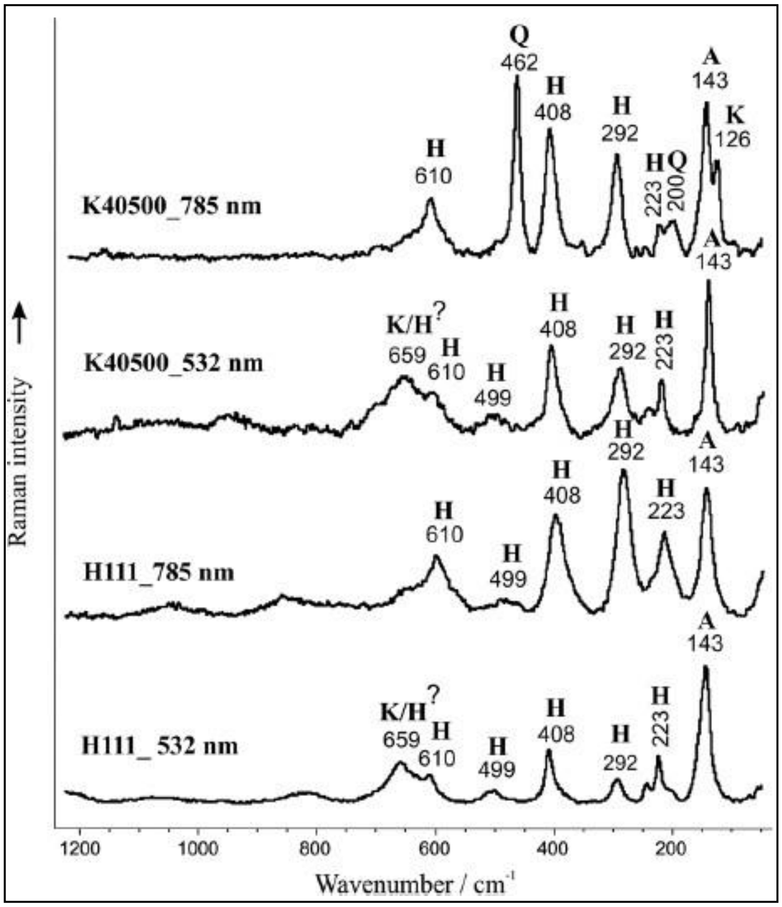

Figure 6.10: Raman spectra of red earths from Hořenec, Czech Republic (H111) and from Bavaria (K40500) at different excitation wavelengths (A = anatase, H = hematite, K = kaolinite, Q = quartz). Image adapted from Košařová et al. [34]

Also, Anatase was present in several of the analyzes with its strong band at 143 cm^{-1} (See Figure 6.9 and Figure 6.10). In our case, analysis is based on the weaker band at 396 cm^{-1} and the very weak band at 196 cm^{-1}.

This relationship perspective regarding Raman spectra analyzes allows us to understand that there are conditions and parameters that may be associated with cultures and sites around the world. The results of different analyzes have similarities with archaeological objects from different sites of the earth. Both samples *M140* and *K40500*[34] are red clay samples that were found in Germany and have compound relationships hundreds of kilometers away. Due to the red pigments of the samples of both works the analysis can be developed in function to understand the similarity of the provenance of this colours.

The importance of the similarity of the compounds and elements of the samples analyzed in Germany by Košařová 34 and the analyzes of this work allows us to understand the similarity that cultures separated by thousands of kilometers have. A comparison among the spectra of the both works samples has been carried out, in order to point out how the relative abundance of certain chemical elements does have clear effects on the shape and intensity of the Raman bands of the clayssy phase.

These similarities provide us with essential characteristics to associate the similarity of elements that exist in areas of different parts of the world and how the different cultures knew how to use them to make different useful objects for their survival.

This work is important for Caranqui, Imbabura and Ecuador due to the contribution it provides to archaeology. Due to these analyzes we can understand certain anthropological behaviors of the ancestral cultures of our country. The study of the origin of the different objects found in Ecuador can give us a better perspective of the life of our ancestors. These works give a very significant importance to the archeometric investigation of Imbabura. This work promotes the analysis of other archaeological pieces in future projects within archaeometry in Ecuador.

Chapter 7

Conclusions

This thesis was conceived to be an “exploration” in the domain of application of Raman spectroscopy as a necessary tool for the non-destructive study of cultural heritage namely ancient pottery. While the use of this technique is well established for the analysis of historic clay objects and pigments, its application to the contribution for the reconstruction of history is recent and still an expanding field.

In this work, the study developed using Raman spectroscopy technique of four vessels from the Caranqui-Inca period was successfully performed. Raman spectroscopy proved a unique tool to investigate the development of studies of ancient pottery without a destruction or invasion of the object. This study also allowed reasserting how careful the researcher should be when attempting to take the samples or manipulate the different instruments.

These analyzes were performed using a Raman spectrometer, different software for their respective information processing. Raman analyses confirm the provenance of the four vessels belonging to the Caranqui-Inca period. The results of the analyzes allow us to infer that the vessels belonged to the same manufacturing period since they contain similar spectral characteristics. The four vessels contain spectral peaks that are in agreement, in addition, they allow us to affirm characteristics of the materials that were used in the Caranqui-Inca period. Knowing the composition of these vessels gives us a guide to understand that they belonged to certain settlements near the Tolas located in the ancient Caranqui country.

The results of samples 1-1CLAY, 2-1CLAY, 3-1CLAY and 4-1CLAY have similarities in their peaks. Certain compounds are not present, but this information tells us that it may have passed through certain environmental conditions or was manufactured with other mixtures of materials. In general, the fact that we have similar materials in the analysis shows us that they were made nearby, or at least, the materials used were obtained from a nearby deposit. These deposits must contain large amounts of albite, anatase, quartz, calcite, hematite and compounds derived from iron-based pigments.

Respect to our findings, for the improve of this kind of analysis the best laser wavelength for differentiation of clay minerals is 1064 nm. Fluorescence in this type of study is a problem that we must try to avoid in order to improve our research. According to Košařová, Hradil, Němec, Bezdička and Kanický[34], if the iron is present directly in the structure of clay minerals (green earths), their near infrared excited Raman spectra are affected by high fluorescence which is probably caused by the ability of near infrared radiation to excite iron atoms.

This technique gives us a mechanism to improve the archaeological study of ancient pottery and art in our country. Raman spectroscopy gives us important information that we can relate to other studies in order to understand historical processes that have not been studied yet. These studies allow us to understand more closely the behavior of ancient cultures that existed here in Ecuador and in other countries such as Germany. Is very interesting the relationship between cultures that lived hundreds of years ago in very distant areas of the planet.

These type of studies are very important because it provides us with information that may be essential to understand the behavior and actions of our ancestors. These types of techniques allow our roots to be explored scientifically. In Ecuador, more studies are needed with different spectroscopy techniques such as Raman. This study follows the path designed by many researchers in the past few years, towards the classification of Raman signatures of cultural heritage materials in the world. Now, it is important to start improving our own path in our country.

Bibliography

[1] Janssens, K., & Van Grieken, R. (2004). *Non-destructive Micro Analysis of Cultural Heritage Materials.* Elsevier.

[2] Smith, Gregory D.; Clark, Robin J.H. (2001). *Raman microscopy in art history and conservation science. Studies in Conservation*, 46(Supplement-1), 92–106. doi:10.1179/sic.2001.46.supplement-1.92

[3] Medeghini, Laura; Mignardi, Silvano; De Vito, Caterina; Bersani, Danilo; Lottici, Pier Paolo; Turetta, Mariangela; Costantini, Jennifer; Bacchini, Elena; Sala, Maura; Nigro, Lorenzo (2013). *The key role of micro-Raman spectroscopy in the study of ancient pottery: the case of pre-classical Jordanian ceramics from the archaeological site of Khirbet al-Batrawy.* European Journal of Mineralogy, 25(5), 881–893. doi:10.1127/0935-1221/2013/0025-2332

[4] Ricciardi, P. (2008). *Raman spectroscopy for the non-destructive characterization of ancient pottery, porcelains and mosaic glasses.* Università degli Studi di Firenze.

[5] Bersani, Danilo; Madariaga, Juan Manuel (2012). *Applications of Raman spectroscopy in art and archaeology.* Journal of Raman Spectroscopy, 43(11), 1523–1528. doi:10.1002/jrs.4219

[6] Vandenabeele, Peter; Edwards, Howell G. M.; Moens, Luc (2007). *A Decade of Raman Spectroscopy in Art and Archaeology.* Chemical Reviews, 107(3), 675–686. doi:10.1021/cr068036i

[7] Bersani, D., Conti, C., Matousek, P., Pozzi, F., & Vandenabeele, P. (2016). *Methodological evolutions of Raman spectroscopy in art and archaeology. Analytical Methods, 8(48), 8395–8409.* doi:10.1039/c6ay02327d

[8] Ludovic Bellot-Gurlet; Sandrine Pagès-Camagna; Claude Coupry (2006). *Raman spectroscopy in art and archaeology*. 37(10), 962–965. doi:10.1002/jrs.1615

[9] Eugenia P. Tomasini; Emilia B. Halac; María Reinoso; Emiliano J. Di Liscia; Marta S. Maier (2012). *Micro-Raman spectroscopy of carbon-based black pigments*. doi:10.1002/jrs.4159

[10] Edwards, Howell G. M.; Vandenabeele, Peter (2016). *Raman spectroscopy in art and archaeology.* Philosophical Transactions of the Royal Society A: Mathematical, Physical and Engineering Sciences, 374(2082), 20160052–. doi:10.1098/rsta.2016.0052

[11] Smith G. D., Clark R. J. H. (2001). *Raman microscopy in art history and conservation science.* Reviews in Conservation, 2, 96–110.

[12] Colomban, Philippe (2013). *The Destructive/Non-Destructive Identification of Enameled Pottery, Glass Artifacts and Associated Pigments*: *A Brief Overview*. Arts, 2(3), 77–110. doi:10.3390/arts2030077

[13] John R. Ferraro, Kazuo Nakamoto, Chris W. Brown. (2003). *Introductory Raman Spectroscopy.* (2nd Edition). Elsevier.

[14] Kuzmany H. (2009). *Solid-State Spectroscopy.* (2nd ed.) Springer.

[15] Larkin P. (2011) *Infrared and Raman Spectroscopy: Principles and spectral interpretation.* Elsevier.

[16] Zeldin, Martel (1966). *An introduction to molecular symmetry and symmetry point groups.* Journal of Chemical Education, 43(1), 17–. doi:10.1021/ed043p17

[17] Rodriguez Ceja, M., Goguitchaichvili, A., Morales, J., Ostrooumov, M., Manzanilla, L. R., Aguilar Reyes, B., & Urrutia-Fucugauchi, J. (2009). *Integrated archeomagnetic and micro–Raman spectroscopy study of pre-Columbian ceramics from the Mesoamerican formative village of Cuanalan, Teotihuacan Valley, Mexico.* Journal of Geophysical Research, 114(B4). doi:10.1029/2008jb006106

[18] Clark, R. J. H., Wang, Q., & Correia, A. (2007). *Can the Raman spectrum of anatase in artwork and archaeology be used for dating purposes? Identification by Raman microscopy of anatase in decorative coatings on Neolithic (Yangshao) pottery from Henan, China.* Journal of Archaeological Science, 34(11), 1787–1793. doi:10.1016/j.jas.2006.12.018

[19] De Faria, D. L. A., & Lopes, F. N. (2007). *Heated goethite and natural hematite: Can Raman spectroscopy be used to differentiate them?* Vibrational Spectroscopy, 45(2), 117–121. doi:10.1016/j.vibspec.2007.07.003

[20] Sánchez-Polo, A., Briceño, S., Jamett, A., Galeas, S., Campaña, O., Guerrero, V., Serrano, J. (2019). *An Archaeometric Characterization of Ecuadorian Pottery.* Scientific Reports, 9(1). doi:10.1038/s41598-018-38293-w

[21] Prinsloo, L. C., Tournié, A., Colomban, P., Paris, C., & Bassett, S. T. (2013). *In search of the optimum Raman/IR signatures of potential ingredients used in San/Bushman rock art paint.* Journal of Archaeological Science, 40(7), 2981–2990.

doi:10.1016/j.jas.2013.02.010

[22] Casanova Municchia, A., Micheli, M., Ricci, M. A., Toledo, M., Bellatreccia, F., Lo Mastro, S., & Sodo, A. (2016). *Raman, SEM–EDS and XRPD investigations on pre-Columbian Central America "estucado" pottery.* Spectrochimica Acta Part A: Molecular and Biomolecular Spectroscopy, 156, 47–53. doi:10.1016/j.saa.2015.11.023

[23] Sendova, Mariana & Zhelyaskov, V. & Scalera, M. & Ramsey, M. (2005). *Micro- Raman spectroscopic study of pottery fragments from the Lapatsa Tomb, Cyprus, ca 2500 BC.* Journal of Raman Spectroscopy. 36. 829 - 833. 10.1002/jrs.1371.

[24] Athens, J. S. 1980. *El Proceso Evolutivo de las Sociedades Complejas y la Ocupación del Período Tardío-Cara en los Andes Septentrionales del Ecuador. Colección Pendoneros,* No. 2. Otavalo, Instituto Otavaleno de Antropologia.

[25] Athens, J. S. 2003. *Inventory of Earthen Mound Sites, Northern Highland Ecuador.* Manuscript on file, National Institute of Cultural Patrimony, Quito.

[26] Sestak, M., Mamedov, S., & Tuschel, D. (s.f.). HORIBA. From Horiba Scientific: https://www.horiba.com/int/products/detail/action/show/Product/xploratm-plus-1528/

[27] Zhou, Zhifei; Li, Chun; He, Tianyin; Lan, Changyong; Sun, Peihua; Zheng, You; Yin, Yi; Liu, Yong (2018). *Facile large-area autofocusing Raman mapping system for 2D material characterization.* Optics Express, 26(7), 9071–. doi:10.1364/oe.26.009071

[28] Brown, R. (1980). PeakFit (Nº de versión v4.12). Windows. Systat Software Inc.

[29] Bray, T. L., & Almeida, J. E. (2014). *The late imperial site of Inca-Caranqui, northern highland Ecuador: at the end of empire.* Ñawpa Pacha, 34(2), 177–199. doi:10.1179/0077629714z.00000000020

[30] Atienza, Lope de 1931 [ca. 1575] *Compendio histórica del estado de los indios del Perú. In La religión del imperio de los Incas,* edited by Jacinto Jijón y Caamaño. Escuela Tipográfica Salesiana, Quito.

[31] Frost, R. L.; Kristof, J. *Clay surfaces: fundamental and applications*; Elsevier, 2004; pp 184–215.

[32] Michaelian, K. H. (1986). *The Raman spectrum of kaolinite #9 at 21°C.* Canadian Journal of Chemistry, 64(2), 285–294. doi:10.1139/v86-048

[33] Sendova, Mariana & Zhelyaskov, V. & Scalera, M. & Ramsey, M. (2005). *Micro- Raman*

spectroscopic study of pottery fragments from the Lapatsa Tomb, Cyprus, ca 2500 BC. Journal of Raman Spectroscopy. 36. 829 - 833. 10.1002/jrs.1371.

[34] Košařová, Veronika & Hradil, David & Nemec, Ivan & Bezdicka, Petr. (2013). *Microanalysis of clay-based pigments in painted artworks by the means of Raman spectroscopy*. Journal of Raman Spectroscopy. 44. 10.1002/jrs.4381.

[35] Nelson, S. (26 de 02 de 2022). Tulane University. Obtenido de Earth & Environmental Sciences 1110: https://www.tulane.edu/~sanelson/eens1110/index.html

[36] Cromer, Don T.; Herrington, K. (1955). *The Structures of Anatase and Rutile.* Journal of the American Chemical Society, 77(18), 4708–4709. doi:10.1021/ja01623a004

[37] Freeman J, Wang A, Kuebler E, Haskin L. Lunar and Planetary Science XXXIV, Houston, TX, 2003; Abstract 1676; http://www.lpi.usra.edu/meetings/lpsc2003/pdf/1676.pdf.

[38] Williams Q. *In A Handbook of Physical Constants: Mineral Physics and Crystallography*, vol. 2, Ahrens TJ (ed). American Geophysical Union: Washington, DC, 1995; 291.

[39] T. P. Mernagh (1991). *Use of the laser Raman microprobe for discrimination amongst feldspar minerals.* 22(8), 453–457. doi:10.1002/jrs.1250220806

[40] Striova, J., Lofrumento, C., Zoppi, A., & Castellucci, E. M. (2006). *Prehistoric Anasazi ceramics studied by micro-Raman spectroscopy.* Journal of Raman Spectroscopy, 37(10), 1139–1145. https://doi.org/10.1002/JRS.1577

[41] Yin, ; Yin, ; Wu, ; Qi, ; Tian, ; Zhang, ; Hu, ; Feng, (2019). *Characterization of coals and coal ashes with high Si content using combined second-derivative Infrared Spectroscopy and Raman Spectroscopy.* Crystals, 9(10), 513–. doi:10.3390/cryst9100513

[42] Striova, J., Lofrumento, C., Zoppi, A., & Castellucci, E. M. (2006). *Prehistoric Anasazi ceramics studied by micro-Raman spectroscopy.* Journal of Raman Spectroscopy, 37(10), 1139–1145. https://doi.org/10.1002/JRS.1577

[43] Noble, J.V. (1960). *The Technique of Attic Vase-Painting.* American Journal of Archaeology, 64, 307 - 318.

[44] Trąbska, J., Wesełucha-Birczyńska, A., Trybalska, B., Przybyła, M., & Byrska- Fudali, M. (2016). *Raman microspectroscopy and SEM/EDS in the investigation of white and red painting layers from Celtic pottery from a Modlniczka site in Poland.* Vibrational Spectroscopy, 86, 233–243. https://doi.org/10.1016/J.VIBSPEC.2016.06.015

[45] Striova, J., Lofrumento, C., Zoppi, A., & Castellucci, E. M. (2006). *Prehistoric Anasazi ceramics studied by micro-Raman spectroscopy*. Journal of Raman Spectroscopy, 37(10), 1139–1145. https://doi.org/10.1002/JRS.1577

[46] Hradil, David & Matys Grygar, Tomas & Hradilová, Janka & Bezdicka, Petr. (2003). *Clay and iron pigments in the history of painting.* Applied Clay Science. 22. 223-236. 10.1016/S0169-1317(03)00076-0.

[47] Herscher E. *In Proceedings of the 3rd International Conference of Cypriot Studies, Nicosia, 3–4 May 1996: Representational Relief on Early and Middle Cypriot Pottery.* Karageorghis V, Laffineur R, Vandenabeele F (eds)A. G. Levantis Foundation: Brussels Liege-Nicosia.